Adaptive IGAFEM with optimal convergence rates

T-splines

Gantner, G.; Praetorius, D.

DOI
10.1016/j.cagd.2020.101906
Publication date
2020
Document Version
Final published version
Published in
Computer Aided Geometric Design

Computer Aided Geometric Design 81 (2020) 101906

Contents lists available at ScienceDirect

Computer Aided Geometric Design

www.elsevier.com/locate/cagd

Adaptive IGAFEM with optimal convergence rates: T-splines ☆

Gregor Gantner [a,*], Dirk Praetorius [b]

[a] Korteweg–de Vries Institute for Mathematics, University of Amsterdam, P.O. Box 94248, 1090 GE Amsterdam, the Netherlands
[b] Institute for Analysis and Scientific Computing, TU Wien, Wiedner Hauptstraße 8-10, A-1040 Wien, Austria

ARTICLE INFO

Article history:
Received 1 October 2019
Received in revised form 20 March 2020
Accepted 29 May 2020
Available online 9 June 2020

Keywords:
Isogeometric analysis
T-splines
Adaptivity
Optimal convergence rates

ABSTRACT

We consider an adaptive algorithm for finite element methods for the isogeometric analysis (IGAFEM) of elliptic (possibly non-symmetric) second-order partial differential equations. We employ analysis-suitable T-splines of arbitrary odd degree on T-meshes generated by the refinement strategy of Morgenstern and Peterseim (2015) in 2D and Morgenstern (2016) in 3D. Adaptivity is driven by some weighted residual *a posteriori* error estimator. We prove linear convergence of the error estimator (which is equivalent to the sum of energy error plus data oscillations) with optimal algebraic rates with respect to the number of elements of the underlying mesh.

1. Introduction

1.1. Adaptivity in isogeometric analysis

The central idea of isogeometric analysis (IGA) (Hughes et al., 2005; Cottrell et al., 2009; Bazilevs et al., 2006) is to use the same ansatz functions for the discretization of the partial differential equation (PDE) as for the representation of the problem geometry in computer aided design (CAD). While the CAD standard for spline representation in a multivariate setting relies on tensor-product B-splines, several extensions of the B-spline model have emerged to allow for adaptive refinement, e.g., (analysis-suitable) T-splines (Sederberg et al., 2003; Dörfel et al., 2010; Scott et al., 2012; Beirão da Veiga et al., 2013), hierarchical splines (Vuong et al., 2011; Giannelli et al., 2012; Kuru et al., 2014), or LR-splines (Dokken et al., 2013; Johannessen et al., 2014); see also (Johannessen et al., 2015; Hennig et al., 2017) for a comparison of these approaches. All these concepts have been studied via numerical experiments. However, to the best of our knowledge, the thorough mathematical analysis of adaptive isogeometric finite element methods (IGAFEM) is so far restricted to hierarchical splines (Buffa and Giannelli, 2016, 2017; Gantner et al., 2017; Buffa and Garau, 2018; Bracco et al., 2019). Recently, linear convergence at optimal algebraic rate with respect to the number of mesh elements has been proved in (Buffa and Giannelli, 2017) for the refinement strategy of (Buffa and Giannelli, 2016) based on truncated hierarchical B-splines (Giannelli et al., 2012), and in our own work (Gantner et al., 2017) for a newly proposed refinement strategy based on standard hierarchical B-splines. In the latter work, we identified certain abstract properties for the underlying meshes, the mesh-refinement, and the finite element spaces that imply well-posedness, reliability, and efficiency of a residual *a posteriori* error estimator and guarantee linear convergence at optimal rate for a related adaptive mesh-refining algorithm. Moreover, in (Gantner et al., 2017) we verified these properties in the case of hierarchical splines. We stress that adaptivity is well understood for

☆ Editor: Oleg Davydov.

* Corresponding author.
E-mail addresses: G.Gantner@uva.nl (G. Gantner), Dirk.Praetorius@asc.tuwien.ac.at (D. Praetorius).

https://doi.org/10.1016/j.cagd.2020.101906

standard FEM with globally continuous piecewise polynomials; see, e.g., (Dörfler, 1996; Morin et al., 2000; Binev et al., 2004; Stevenson, 2007; Cascon et al., 2008; Feischl et al., 2014; Carstensen et al., 2014) for milestones on convergence and optimal convergence rates. In the frame of adaptive isogeometric boundary element methods (IGABEM), we also mention our recent works (Feischl et al., 2015, 2016, 2017; Gantner, 2017; Gantner et al., 2020a).

1.2. Model problem

On the bounded Lipschitz domain $\Omega \subset \mathbb{R}^d$, $d \in \{2, 3\}$, with initial mesh $\mathcal{T}_0$ and for given $f \in L^2(\Omega)$ as well as $\boldsymbol{f} \in L^2(\Omega)^d$ with $\boldsymbol{f}|_T \in \boldsymbol{H}(\mathrm{div}, T)$ for all $T \in \mathcal{T}_0$, we consider a general second-order linear elliptic PDE in divergence form with homogenous Dirichlet boundary conditions

$$\begin{aligned} \mathcal{L}u := -\mathrm{div}(\boldsymbol{A}\nabla u) + \boldsymbol{b}\cdot\nabla u + cu = f + \mathrm{div}\,\boldsymbol{f} \quad &\text{in } \Omega, \\ u = 0 \quad &\text{on } \partial\Omega. \end{aligned} \tag{1.1}$$

We pose the following regularity assumptions on the coefficients: $\boldsymbol{A}(x) \in \mathbb{R}^{d\times d}_{\mathrm{sym}}$ is a symmetric and uniformly positive definite matrix with $\boldsymbol{A} \in L^\infty(\Omega)^{d\times d}$ and $\boldsymbol{A}|_T \in W^{1,\infty}(T)$ for all $T \in \mathcal{T}_0$. The vector $\boldsymbol{b}(x) \in \mathbb{R}^d$ and the scalar $c(x) \in \mathbb{R}$ satisfy that $\boldsymbol{b}, c \in L^\infty(\Omega)$. We interpret $\mathcal{L}$ in its weak form and define the corresponding bilinear form

$$\langle w\,,\, v\rangle_{\mathcal{L}} := \int_\Omega \boldsymbol{A}(x)\nabla w(x)\cdot\nabla v(x) + \boldsymbol{b}(x)\cdot\nabla w(x)\, v(x) + c(x)\, w(x)\, v(x)\, dx. \tag{1.2}$$

The bilinear form is continuous, i.e., it holds that

$$\langle w\,,\, v\rangle_{\mathcal{L}} \le \big(\|\boldsymbol{A}\|_{L^\infty(\Omega)} + \|\boldsymbol{b}\|_{L^\infty(\Omega)} + \|c\|_{L^\infty(\Omega)}\big)\|w\|_{H^1(\Omega)}\|v\|_{H^1(\Omega)} \quad \text{for all } v, w \in H^1(\Omega). \tag{1.3}$$

Additionally, we suppose ellipticity of $\langle\cdot\,,\,\cdot\rangle_{\mathcal{L}}$ on $H^1_0(\Omega)$, i.e.,

$$\langle v\,,\, v\rangle_{\mathcal{L}} \ge C_{\mathrm{ell}}\|v\|^2_{H^1(\Omega)} \quad \text{for all } v \in H^1_0(\Omega). \tag{1.4}$$

Note that (1.4) is for instance satisfied if $\boldsymbol{A}(x)$ is uniformly positive definite and if $\boldsymbol{b} \in \boldsymbol{H}(\mathrm{div}, \Omega)$ with $-\frac{1}{2}\,\mathrm{div}\,\boldsymbol{b}(x) + c(x) \ge 0$ almost everywhere in Ω.

Overall, the boundary value problem (1.1) fits into the setting of the Lax–Milgram theorem and therefore admits a unique solution $u \in H^1_0(\Omega)$ to the weak formulation

$$\langle u\,,\, v\rangle_{\mathcal{L}} = \int_\Omega f v - \boldsymbol{f}\cdot\nabla v\, dx \quad \text{for all } v \in H^1_0(\Omega). \tag{1.5}$$

Finally, we note that the additional regularity $\boldsymbol{f}|_T \in \boldsymbol{H}(\mathrm{div}, T)$ and $\boldsymbol{A}|_T \in W^{1,\infty}(T)$ for all $T \in \mathcal{T}_0$ is only required for the well-posedness of the residual *a posteriori* error estimator; see Section 2.5.

1.3. Outline & contributions

The remainder of this work is organized as follows: Section 2 recalls the definition of T-meshes and T-splines of arbitrary odd degree in the parameter domain (Section 2.1) from (Beirão da Veiga et al., 2013) for $d = 2$ and from (Morgenstern, 2016)[1] for $d = 3$. Moreover, it recalls corresponding refinement strategies (Section 2.2) from (Morgenstern and Peterseim, 2015; Morgenstern, 2016), derives a canonical basis for the T-spline space with homogeneous boundary conditions (Section 2.3), and transfers all the definitions to the physical domain Ω via some parametrization $\gamma : [0, 1]^d \to \overline{\Omega}$ (Section 2.4). Subsequently, we formulate a standard adaptive algorithm (Algorithm 2.7) of the form

$$\boxed{\texttt{solve}} \longrightarrow \boxed{\texttt{estimate}} \longrightarrow \boxed{\texttt{mark}} \longrightarrow \boxed{\texttt{refine}} \tag{1.6}$$

driven by some residual *a posteriori* error estimator (2.37). For T-splines in 2D, this algorithm has already been investigated numerically in (Hennig et al., 2017). Finally, our main result Theorem 2.11 is presented. First, it states that the error estimator η_ℓ associated with the FEM solution $U_\ell \in \mathcal{X}_\ell \subset H^1_0(\Omega)$ is efficient and reliable, i.e., there exist C_{eff}, $C_{\mathrm{rel}} > 0$ such that

$$C_{\mathrm{eff}}^{-1}\,\eta_\ell \le \inf_{V_\ell\in\mathcal{X}_\ell}\big(\|u - V_\ell\|_{H^1(\Omega)} + \mathrm{osc}_\ell(V_\ell)\big) \le \|u - U_\ell\|_{H^1(\Omega)} + \mathrm{osc}_\ell(U_\ell) \le C_{\mathrm{rel}}\,\eta_\ell, \tag{1.7}$$

[1] To be precise, we define T-splines for $d = 3$ slightly different than (Morgenstern, 2016); see Section 2.3 for details.

where η_ℓ denotes the error estimator in the ℓ-th step of the adaptive algorithm and $\operatorname{osc}_\ell(\cdot)$ denotes the corresponding data oscillation terms (see (2.41)). Second, it states that Algorithm 2.7 leads to linear convergence with optimal rates in the spirit of (Stevenson, 2007; Cascon et al., 2008; Carstensen et al., 2014): There exist $C > 0$ and $0 < q < 1$ such that

$$\eta_{\ell+j} \le C\, q^j\, \eta_\ell \quad \text{for all } \ell, j \in \mathbb{N}_0. \tag{1.8}$$

Moreover, for sufficiently small marking parameters in Algorithm 2.7, the estimator (and thus equivalently also the so-called total error $\|u - U_\ell\|_{H^1(\Omega)} + \operatorname{osc}_\ell(U_\ell)$; see (1.7)) decays even with the optimal algebraic convergence rate with respect to the number of mesh elements, i.e.,

$$\eta_\ell = \mathcal{O}\big((\#\mathcal{T}_\ell)^{-s}\big) \quad \text{for all } \ell \in \mathbb{N}_0, \tag{1.9}$$

whenever the rate $s > 0$ is possible for optimally chosen meshes. The proof of Theorem 2.11 is postponed to Section 3 and is based on abstract properties of the underlying meshes, the mesh-refinement, the finite element spaces, and the oscillations which have been identified in (Gantner et al., 2017) and imply (an abstract version of) Theorem 2.11. In Section 3, we briefly recapitulate these properties and verify them for the present T-spline setting. The final Section 4 comments on possible extensions of Theorem 2.11.

1.4. General notation

Throughout, $|\cdot|$ denotes the absolute value of scalars, the Euclidean norm of vectors in $\mathbb{R}^d$, and the d-dimensional measure of a set in $\mathbb{R}^d$. Moreover, # denotes the cardinality of a set as well as the multiplicity of a knot within a given knot vector. We write $A \lesssim B$ to abbreviate $A \le C B$ with some generic constant $C > 0$, which is clear from the context. Moreover, $A \simeq B$ abbreviates $A \lesssim B \lesssim A$. Throughout, mesh-related quantities have the same index, e.g., $\mathcal{X}_\bullet$ is the ansatz space corresponding to the mesh $\mathcal{T}_\bullet$. The analogous notation is used for meshes $\mathcal{T}_\circ$, $\mathcal{T}_\star$, $\mathcal{T}_\ell$ etc. Moreover, we use $\widehat{\cdot}$ to transfer quantities in the physical domain Ω to the parameter domain $\widehat{\Omega}$, e.g., we write $\widehat{\mathbb{T}}$ for the set of all admissible meshes in the parameter domain, while $\mathbb{T}$ denotes the set of all admissible meshes in the physical domain.

2. Adaptivity with T-splines

In this section, we recall the formal definition of T-splines from (Beirão da Veiga et al., 2013) for $d = 2$ and from (Morgenstern, 2016) for $d = 3$ as well as corresponding mesh-refinement strategies from (Morgenstern and Peterseim, 2015; Morgenstern, 2016). While the mathematically sound definition is a bit tedious, the basic idea of T-splines is simple: Given a rectangular mesh (with hanging nodes) as in Fig. 2.3, one associates to all nodes a local knot vector in each direction as the intersections (projected into the white area $\overline{\widehat{\Omega}}$) of the line in that direction through the node (indicated in red) with the mesh skeleton. The resulting local knot vectors then induce a standard tensor-product B-spline, and the set of all such B-splines spans the corresponding T-spline space. Moreover, we formulate an adaptive algorithm (Algorithm 2.7) for conforming FEM discretizations of our model problem (1.1), where adaptivity is driven by the residual *a posteriori* error estimator (see (2.37) below). Our main result of the present work Theorem 2.11 states reliability and efficiency of the estimator as well as linear convergence at optimal algebraic rate with respect to the number of mesh elements.

2.1. T-meshes and T-splines in the parameter domain $\widehat{\Omega}$

Meshes $\mathcal{T}_\bullet$ and corresponding spaces $\mathcal{X}_\bullet$ are defined through their counterparts on the *parameter domain*

$$\widehat{\Omega} := (0, N_1) \times \cdots \times (0, N_d), \tag{2.1}$$

where $N_i \in \mathbb{N}$ are fixed integers for $i \in \{1, \dots, d\}$. Recall that the symbol $\bullet$ is used for a generic mesh index to relate corresponding quantities; see the general notation of Section 1.4. Let $p_1, \dots, p_d \ge 3$ be fixed odd polynomial degrees. Let $\widehat{\mathcal{T}}_0$ be an initial uniform tensor-mesh of the form

$$\widehat{\mathcal{T}}_0 = \Big\{ \prod_{i=1}^d [a_i, a_i + 1] : a_i \in \{0, \dots, N_i - 1\} \text{ for } i \in \{1, \dots, d\} \Big\}. \tag{2.2}$$

For an arbitrary hyperrectangle $\widehat{T} = [a_1, b_1] \times \dots [a_d, b_d]$, we define its bisection in direction $i \in \{1, \dots, d\}$ as the set

$$\begin{aligned} \texttt{bisect}_i(\widehat{T}) := \Big\{ &\prod_{j=1}^{i-1} [a_j, b_j] \times \Big[a_i, \frac{a_i + b_i}{2}\Big] \times \prod_{j=i+1}^{d} [a_j, b_j], \\ &\prod_{j=1}^{i-1} [a_j, b_j] \times \Big[\frac{a_i + b_i}{2}, b_i\Big] \times \prod_{j=i+1}^{d} [a_j, b_j] \Big\}. \end{aligned} \tag{2.3}$$

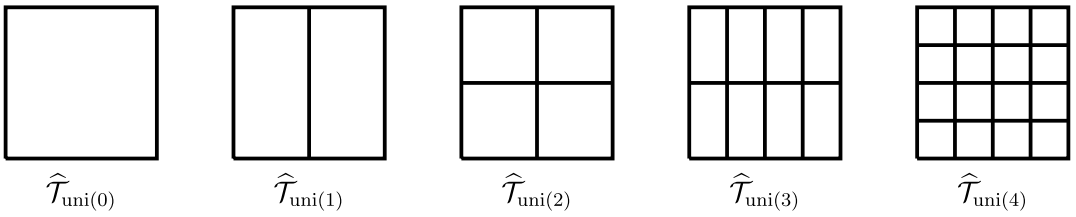

Fig. 2.1. Uniform refinements of 2D initial partition $\widehat{\mathcal{T}}_0 := \{[0,1]^2\}$.

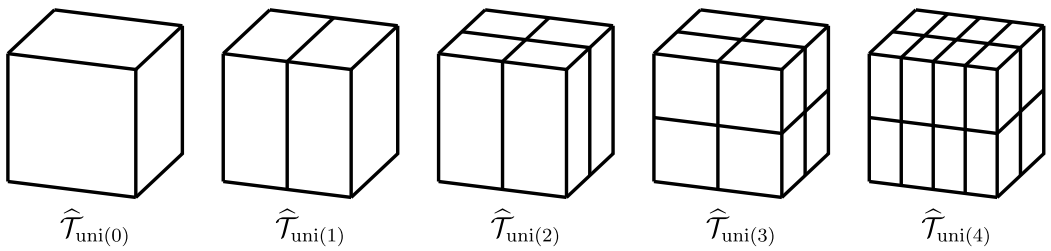

Fig. 2.2. Uniform refinements of 3D initial partition $\widehat{\mathcal{T}}_0 := \{[0,1]^3\}$.

For $k \in \mathbb{N}_0$, let

$$\underline{k} := \lfloor k/d \rfloor d \tag{2.4}$$

and define the k-th uniform refinement of $\widehat{\mathcal{T}}_0$ inductively by

$$\widehat{\mathcal{T}}_{\mathrm{uni}(0)} := \widehat{\mathcal{T}}_0 \quad \text{and} \quad \widehat{\mathcal{T}}_{\mathrm{uni}(k)} := \bigcup \big\{ \mathtt{bisect}_{k+1-\underline{k}}(\widehat{T}) : \widehat{T} \in \widehat{\mathcal{T}}_{\mathrm{uni}(k-1)} \big\}; \tag{2.5}$$

see Fig. 2.1 and 2.2. Note that the direction of bisection changes periodically.

A finite set $\widehat{\mathcal{T}}_\bullet$ is a *T-mesh (in the parameter domain)*, if $\widehat{\mathcal{T}}_\bullet \subseteq \bigcup_{k\in\mathbb{N}_0} \widehat{\mathcal{T}}_{\mathrm{uni}(k)}$, $\bigcup_{\widehat{T}\in\widehat{\mathcal{T}}_\bullet} \widehat{T} = \overline{\widehat{\Omega}}$, and $|\widehat{T} \cap \widehat{T}'| = 0$ for all $\widehat{T}, \widehat{T}' \in \widehat{\mathcal{T}}_\bullet$ with $\widehat{T} \neq \widehat{T}'$. For an illustrative example of a general T-mesh, see Fig. 2.3. Since $\widehat{\mathcal{T}}_{\mathrm{uni}(k)} \cap \widehat{\mathcal{T}}_{\mathrm{uni}(k')} = \emptyset$ for $k, k' \in \mathbb{N}_0$ with $k \neq k'$, each element $\widehat{T} \in \widehat{\mathcal{T}}_\bullet$ has a natural level

$$\mathrm{level}(\widehat{T}) := k \in \mathbb{N}_0 \quad \text{with } \widehat{T} \in \widehat{\mathcal{T}}_{\mathrm{uni}(k)}. \tag{2.6}$$

In order to define T-splines, in particular to allow for knot multiplicities larger than one at the boundary, we have to extend the mesh $\widehat{\mathcal{T}}_\bullet$ on $\overline{\widehat{\Omega}}$ to a mesh on $\overline{\widehat{\Omega}^{\mathrm{ext}}}$, where

$$\widehat{\Omega}^{\mathrm{ext}} := \prod_{i=1}^{d} (-p_i, N_i + p_i). \tag{2.7}$$

We define $\widehat{\mathcal{T}}_0^{\mathrm{ext}}$ analogously to (2.2) and $\widehat{\mathcal{T}}_\bullet^{\mathrm{ext}}$ as the mesh on $\overline{\widehat{\Omega}^{\mathrm{ext}}}$ that is obtained by extending any bisection which takes place on the boundary $\partial\widehat{\Omega}$ during the refinement from $\widehat{\mathcal{T}}_0$ to $\widehat{\mathcal{T}}_\bullet$, to the set $\overline{\widehat{\Omega}^{\mathrm{ext}}} \setminus \overline{\widehat{\Omega}}$; see Fig. 2.3. For $d = 2$, this formally reads

$$\widehat{\mathcal{T}}_\bullet^{\mathrm{ext}} := \widehat{\mathcal{T}}_\bullet \cup \big\{ \mathrm{ext}_\bullet(\widehat{E}_1 \times \widehat{E}_2) : \dim(\widehat{E}_1 \times \widehat{E}_2) < 2 \wedge \widehat{E}_i \in \{\{0\}, \{N_i\}, [0, N_i]\} \text{ for } i \in \{1,2\} \big\}, \tag{2.8}$$

where

$$\begin{aligned} \mathrm{ext}_\bullet\big(\{(0,0)\}\big) &:= \big\{ [a_1, a_1+1] \times [a_2, a_2+1] : a_i \in \{-p_i, \dots, -1\} \text{ for } i \in \{1,2\} \big\}, \\ \mathrm{ext}_\bullet\big([0,N_1] \times \{0\}\big)\big) &:= \big\{ [a_1, b_1] \times [a_2, a_2+1] : a_2 \in \{-p_2, \dots, -1\} \wedge \exists b_2' : [a_1, b_1] \times [0, b_2'] \in \widehat{\mathcal{T}}_\bullet \big\}, \end{aligned}$$

and the remaining $\mathrm{ext}_\bullet(\cdot)$ terms are defined analogously. Note that the logical expression

$$\exists b_2' : [a_1, b_1] \times [0, b_2'] \in \widehat{\mathcal{T}}_\bullet$$

means that there exists an element at the (lower part of the) boundary $\partial\widehat{\Omega}$ with side $[a_1, b_1]$. For $d = 3$, this reads

$$\widehat{\mathcal{T}}_\bullet^{\mathrm{ext}} := \widehat{\mathcal{T}}_\bullet \cup \Big\{ \mathrm{ext}_\bullet\Big(\prod_{i=1}^{3} \widehat{E}_i\Big) : \dim\Big(\prod_{i=1}^{3} \widehat{E}_i\Big) < 3 \wedge \widehat{E}_i \in \{\{0\}, \{N_i\}, [0, N_i]\} \text{ for } i \in \{1,2,3\} \Big\},$$

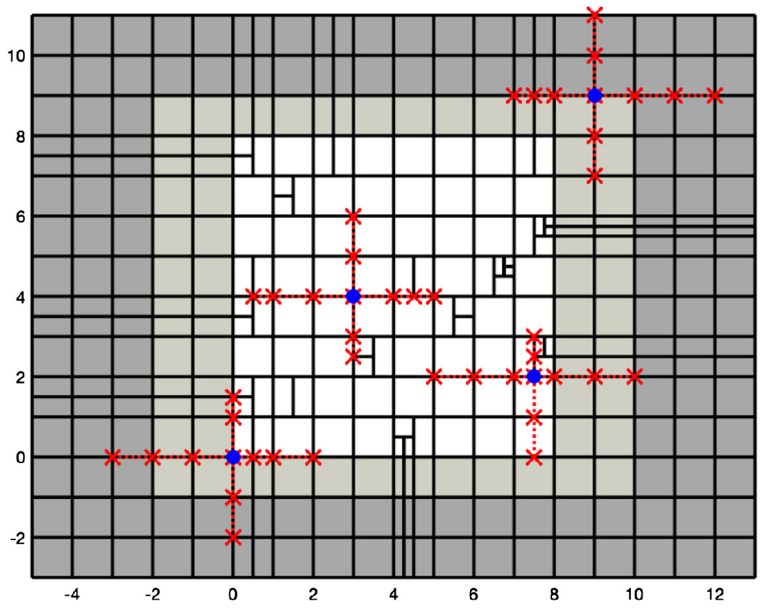

Fig. 2.3. A general (non-admissible) T-mesh $\widehat{\mathcal{T}}_\bullet^{\mathrm{ext}}$ in 2D with $(p_1, p_2) = (5, 3)$ is depicted. The sets $\widehat{\Omega}$, $\widehat{\Omega}^{\mathrm{act}}$, and $\widehat{\Omega}^{\mathrm{ext}}$ are highlighted in white, light gray, and dark gray, respectively. For the three (blue) nodes $z \in \{(0,0), (3,4), (7.5,2), (9,9)\}$, their corresponding local index vectors $\widehat{\mathcal{I}}_{\bullet,i}^{\mathrm{loc}}(z)$ with $i \in \{1,2\}$ are indicated by (red) crosses. We also indicate in red the lines through the nodes mentioned at the beginning of Section 2. The local knot vectors are obtained by setting all negative values to 0 and all values larger than 8 to 8, i.e., $\widehat{\mathcal{K}}_{\bullet,1}^{\mathrm{loc}}\big((0,0)\big) = (0,0,0,0,0.5,1,2)$, $\widehat{\mathcal{K}}_{\bullet,2}^{\mathrm{loc}}\big((0,0)\big) = (0,0,0,1,1.5)$, $\widehat{\mathcal{K}}_{\bullet,1}^{\mathrm{loc}}\big((3,4)\big) = (0.5,1,2,3,4,4.5,5)$, $\widehat{\mathcal{K}}_{\bullet,2}^{\mathrm{loc}}\big((3,4)\big) = (2.5,3,4,5,6)$, $\widehat{\mathcal{K}}_{\bullet,1}^{\mathrm{loc}}\big((7.5,2)\big) = (5,6,7,7.5,8,8,8)$, $\widehat{\mathcal{K}}_{\bullet,2}^{\mathrm{loc}}\big((7.5,2)\big) = (0,1,2,2.5,3)$, $\widehat{\mathcal{K}}_{\bullet,1}^{\mathrm{loc}}\big((9,9)\big) = (7,7.5,8,8,8,8,8)$, $\widehat{\mathcal{K}}_{\bullet,2}^{\mathrm{loc}}\big((9,9)\big) = (7,8,8,8,8)$. This guarantees that all associated B-splines have support within the closure of $\widehat{\Omega}$. (For interpretation of the colors in the figure(s), the reader is referred to the web version of this article.)

where

$$\begin{aligned}
\mathrm{ext}_\bullet\big(\{(0,0,0)\}\big) &:= \Big\{ \prod_{i=1}^{3} [a_i, a_i+1] : a_i \in \{-p_i, \dots, -1\} \text{ for } i \in \{1,2,3\} \Big\},\\
\mathrm{ext}_\bullet\big([0,N_1]\times\{0\}\times\{0\}\big) &:= \big\{ [a_1,b_1]\times[a_2,a_2+1]\times[a_3,a_3+1] :\\
&\qquad a_i \in \{-p_i,\dots,-1\} \text{ for } i\in\{2,3\} \wedge \exists b_2', b_3' : [a_1,b_1]\times[0,b_2']\times[0,b_3'] \in \widehat{\mathcal{T}}_\bullet \big\},\\
\mathrm{ext}_\bullet\big([0,N_1]\times[0,N_2]\times\{0\}\big) &:= \big\{ [a_1,b_1]\times[a_2,b_2]\times[a_3,a_3+1] :\\
&\qquad a_3 \in \{-p_3,\dots,-1\} \wedge \exists b_3' : [a_1,b_1]\times[a_2,b_2]\times[0,b_3'] \in \widehat{\mathcal{T}}_\bullet \big\},
\end{aligned}$$

and the remaining $\mathrm{ext}_\bullet(\cdot)$ terms are defined analogously. Note that the logical expressions

$$\exists b_2', b_3' : [a_1,b_1]\times[0,b_2']\times[0,b_3'] \in \widehat{\mathcal{T}}_\bullet \quad \text{and} \quad \exists b_3' : [a_1,b_1]\times[a_2,b_2]\times[0,b_3'] \in \widehat{\mathcal{T}}_\bullet$$

mean that there exists an element at the (lower part of the) boundary $\partial\widehat{\Omega}$ with side $[a_1,b_1]$, and with sides $[a_1,b_1]$ as well as $[a_2,b_2]$, respectively. The corresponding *skeleton* in any direction $i \in \{1,\dots,d\}$ reads

$$\partial_i \widehat{\mathcal{T}}_\bullet^{\mathrm{ext}} := \bigcup \Big\{ \prod_{j=1}^{i-1} [a_j,b_j] \times \{a_i,b_i\} \times \prod_{j=i+1}^{d} [a_j,b_j] : \prod_{j=1}^{d} [a_j,b_j] \in \widehat{\mathcal{T}}_\bullet^{\mathrm{ext}} \Big\}. \tag{2.9}$$

Recall that $p_i \geq 3$ are odd. We abbreviate

$$\widehat{\Omega}^{\mathrm{act}} := \prod_{i=1}^{d} \big(-(p_i-1)/2, N_i + (p_i-1)/2 \big). \tag{2.10}$$

As in the literature, its closure $\overline{\widehat{\Omega}^{\mathrm{act}}}$ is called *active region*, whereas $\overline{\widehat{\Omega}^{\mathrm{ext}}} \setminus \widehat{\Omega}^{\mathrm{act}}$ is called *frame region*. The set of *nodes* $\widehat{\mathcal{N}}_\bullet^{\mathrm{act}}$ in the active region reads

$$\widehat{\mathcal{N}}_\bullet^{\mathrm{act}} := \big\{ z \in \overline{\widehat{\Omega}^{\mathrm{act}}} : z \text{ is vertex of some } \widehat{T} \in \widehat{\mathcal{T}}_\bullet^{\mathrm{act}} \big\}. \tag{2.11}$$

To each node $z = (z_1, \dots, z_d) \in \widehat{\mathcal{N}}_\bullet^{\mathrm{act}}$ and each direction $i \in \{1, \dots, d\}$, we associate the corresponding *global index vector* which is obtained by drawing a line in the i-th direction through the node z and collecting the i-th coordinates of the intersections with the skeleton. Formally, this reads

$$\widehat{\mathcal{I}}_{\bullet,i}^{\mathrm{gl}}(z) := \mathrm{sort}\big(\big\{t \in [-p_i, N_i + p_i] : (z_1, \dots, z_{i-1}, t, z_{i+1}, \dots, z_d) \in \partial_i \widehat{\mathcal{T}}_\bullet^{\mathrm{ext}}\big\}\big),$$

where $\mathrm{sort}(\cdot)$ returns (in ascending order) the sorted vector corresponding to a set of numbers. The corresponding *local index vector*

$$\widehat{\mathcal{I}}_{\bullet,i}^{\mathrm{loc}}(z) \in \mathbb{R}^{p_i+2} \tag{2.12}$$

is the vector of all $p_i + 2$ consecutive elements in $\widehat{\mathcal{I}}_{\bullet,i}^{\mathrm{gl}}(z)$ having z_i as their $((p_i+3)/2)$-th (i.e., their middle) entry; see Fig. 2.3. Note that such elements always exist due to the definition of $\widehat{\mathcal{I}}_{\bullet,i}^{\mathrm{gl}}(z)$ and the fact that p_i is odd. This induces the *global knot vector*

$$\widehat{\mathcal{K}}_{\bullet,i}^{\mathrm{gl}}(z) := \max\Big(\min\big(\widehat{\mathcal{I}}_{\bullet,i}^{\mathrm{gl}}(z), N_i\big), 0\Big), \tag{2.13}$$

and the *local knot vector*

$$\widehat{\mathcal{K}}_{\bullet,i}^{\mathrm{loc}}(z) := \max\Big(\min\big(\widehat{\mathcal{I}}_{\bullet,i}^{\mathrm{loc}}(z), N_i\big), 0\Big), \tag{2.14}$$

where $\max(\cdot, 0)$ and $\min(\cdot, N_i)$ are understood element-wise (i.e., for each element in $\widehat{\mathcal{I}}_{\bullet,i}^{\mathrm{gl}}(z)$ and $\widehat{\mathcal{I}}_{\bullet,i}^{\mathrm{loc}}(z)$, respectively). We stress that the resulting global knot vectors in each direction are so-called *open knot vectors*, i.e., the multiplicity of the first knot 0 and the last knot N_i is $p_i + 1$. Moreover, the interior knots coincide with the indices in $\widehat{\Omega}$ and all have multiplicity one. For more general index to parameter mappings, we refer to Section 4.2. We define the corresponding tensor-product B-spline $\widehat{B}_{\bullet,z} : \overline{\widehat{\Omega}} \to \mathbb{R}$ as

$$\widehat{B}_{\bullet,z}(t_1, \dots, t_d) := \prod_{i=1}^{d} \widehat{B}\big(t_i \,|\, \widehat{\mathcal{K}}_{\bullet,i}^{\mathrm{loc}}(z)\big) \quad \text{for all } (t_1, \dots, t_d) \in \overline{\widehat{\Omega}}, \tag{2.15}$$

where $\widehat{B}\big(t_i \,|\, \widehat{\mathcal{K}}_{\bullet,i}^{\mathrm{loc}}(z)\big)$ denotes the unique one-dimensional B-spline induced by $\widehat{\mathcal{K}}_{\bullet,i}^{\mathrm{loc}}(z)$. For convenience of the reader, we recall the following definition for arbitrary $p \in \mathbb{N}_0$ via divided differences,[2]

$$\widehat{B}\big(t|(x_0, \dots, x_{p+1})\big) := (x_{p+1} - x_0) \cdot [x_0, \dots, x_{p+1}]\big(\max\{(\cdot) - t, 0\}^p\big) \quad \text{for all } t \in \mathbb{R} \text{ and } x_0 \le \dots \le x_{p+1};$$

see also (de Boor, 2001) for equivalent definitions and elementary properties. We only mention that $\widehat{B}\big(\,\cdot\,|(x_0, \dots, x_{p+1})\big)$ is positive on the open interval (x_0, x_{p+1}), it does not vanish at x_0 if and only if $x_0 = \dots = x_p$, and it does not vanish at x_{p+1} if and only if $x_1 = \dots = x_{p+1}$. Due to definition (2.14), each $\widehat{B}_{\bullet,z}$ has thus indeed only support within the closure of the parameter domain $\widehat{\Omega}$, and multiple knots may only occur at the boundary $\partial\widehat{\Omega}$. According to, e.g., (de Boor, 2001, Section 6), each tensor-product B-spline satisfies that $\widehat{B}_{\bullet,z} \in C^2\big(\overline{\widehat{\Omega}}\big)$. With this, we see for the space of *T-splines in the parameter domain* that

$$\widehat{\mathcal{Y}}_\bullet := \mathrm{span}\big\{\widehat{B}_{\bullet,z} : z \in \widehat{\mathcal{N}}_\bullet^{\mathrm{act}}\big\} \subset C^2\big(\overline{\widehat{\Omega}}\big). \tag{2.16}$$

Finally, we define our ansatz space in the parameter domain as

$$\widehat{\mathcal{X}}_\bullet := \big\{\widehat{V}_\bullet \in \widehat{\mathcal{Y}}_\bullet : \widehat{V}_\bullet|_{\partial\widehat{\Omega}} = 0\big\}. \tag{2.17}$$

Note that this specifies the abstract setting of Section 3.3. For a more detailed introduction to T-meshes and splines, we refer to, e.g., (Beirão da Veiga et al., 2014, Section 7).

2.2. Refinement in the parameter domain $\widehat{\Omega}$

In this section, we recall the refinement algorithm from (Morgenstern and Peterseim, 2015, Algorithm 2.9 and Corollary 2.15) for $d = 2$ and (Morgenstern, 2016, Algorithm 2.9) for $d = 3$; see also (Morgenstern, 2017, Chapter 5). To this end, we first define for a T-mesh $\widehat{\mathcal{T}}_\bullet$ and $\widehat{T} \in \widehat{\mathcal{T}}_\bullet$ with $k := \mathrm{level}(\widehat{T})$ the set of its *neighbors*

$$\mathbf{N}_\bullet(\widehat{T}) := \big\{\widehat{T}' \in \widehat{\mathcal{T}}_\bullet : \exists t \in \widehat{T}' \text{ with } |\mathrm{mid}_i(\widehat{T}) - t_i| < D_i(k) \text{ for all } i \in \{1, \dots, d\}\big\}, \tag{2.18}$$

[2] For any function $F : \mathbb{R} \to \mathbb{R}$, divided differences are recursively defined via $[x_0]F := F(x_0)$ and $[x_0, \dots, x_{j+1}]F := \big([x_1, \dots, x_{j+1}]F - [x_0, \dots, x_j]F\big)/(x_{j+1} - x_0)$ for $j = 0, \dots, p$.

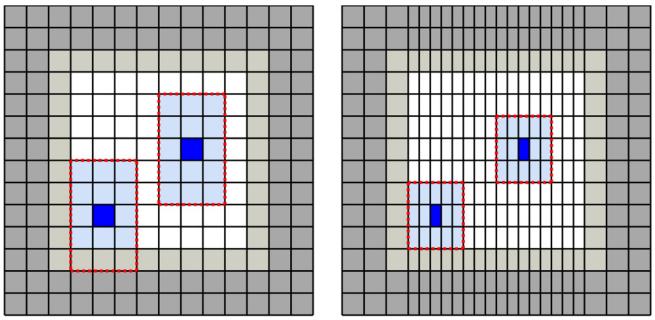

Fig. 2.4. An initial T-mesh $\widehat{\mathcal{T}}_0^{\mathrm{ext}}$ in 2D (left) with $(p_1, p_2) = (3, 3)$ and its first uniform refinement (right) are depicted. The sets $\widehat{\Omega}$, $\widehat{\Omega}^{\mathrm{act}}$, and $\widehat{\Omega}^{\mathrm{ext}}$ are highlighted in white, light gray, and dark gray, respectively. For each of the four blue elements, the corresponding neighbors are shown in light blue. According to definition (2.18), the neighbors are all elements in $\overline{\widehat{\Omega}}$ with non-empty intersection with the rectangles indicated in red.

where $\mathrm{mid}(\widehat{T}) = (\mathrm{mid}_1(\widehat{T}), \dots, \mathrm{mid}_d(\widehat{T}))$ denotes the midpoint of $\widehat{T}$ and $D(k) = (D_1(k), \dots, D_d(k))$ is defined as

$$D(k) := \begin{cases} 2^{-k/2}\big(p_1/2,\ p_2/2+1\big) & \text{if } d=2 \text{ and } k=0 \bmod 2,\\ 2^{-(k-1)/2}\big(p_1/4+1/2,\ p_2/2\big) & \text{if } d=2 \text{ and } k=1 \bmod 2,\\ 2^{-k/3}\big(p_1+3/2,\ p_2+3/2,\ p_3+3/2\big) & \text{if } d=3 \text{ and } k=0 \bmod 3,\\ 2^{-(k-1)/3}\big(p_1/2+3/4,\ p_2+3/2,\ p_3+3/2\big) & \text{if } d=3 \text{ and } k=1 \bmod 3,\\ 2^{-(k-2)/3}\big(p_1/2+3/4,\ p_2/2+3/4,\ p_3+3/2\big) & \text{if } d=3 \text{ and } k=2 \bmod 3; \end{cases} \tag{2.19}$$

see Fig. 2.4 and 2.5 for some examples. For $d = 2$, (Morgenstern and Peterseim, 2015, Corollary 2.15) also provides the following identity

$$\mathbf{N}_\bullet(\widehat{T}) = \big\{\widehat{T}' \in \widehat{\mathcal{T}}_\bullet : |\mathrm{mid}_i(\widehat{T}) - \mathrm{mid}_i(\widehat{T}')| \le D_i(k) \text{ for all } i \in \{1,2\}\big\}. \tag{2.20}$$

We define the set of *bad neighbors*

$$\mathbf{N}_\bullet^{\mathrm{bad}}(\widehat{T}) := \big\{\widehat{T}' \in \mathbf{N}_\bullet(\widehat{T}) : \mathrm{level}(\widehat{T}') < \mathrm{level}(\widehat{T})\big\}. \tag{2.21}$$

Algorithm 2.1. Input: T-mesh $\widehat{\mathcal{T}}_\bullet$, marked elements $\widehat{\mathcal{M}}_\bullet =: \widehat{\mathcal{M}}_\bullet^{(0)} \subseteq \widehat{\mathcal{T}}_\bullet$.

(i) Iterate the following steps (a)–(b) for $j = 0, 1, 2, \dots$ until $\widehat{\mathcal{U}}_\bullet^{(j)} = \emptyset$:

(a) Define $\widehat{\mathcal{U}}_\bullet^{(j)} := \bigcup_{\widehat{T} \in \widehat{\mathcal{M}}_\bullet^{(j)}} \mathbf{N}^{\mathrm{bad}}(\widehat{T}) \setminus \widehat{\mathcal{M}}_\bullet^{(j)}$.

(b) Define $\widehat{\mathcal{M}}_\bullet^{(j+1)} := \widehat{\mathcal{M}}_\bullet^{(j)} \cup \widehat{\mathcal{U}}_\bullet^{(j)}$.

(ii) Bisect all $\widehat{T} \in \widehat{\mathcal{M}}_\bullet^{(j)}$ via $\mathtt{bisect}_{\mathrm{level}(\widehat{T})+1-\underline{\mathrm{level}(\widehat{T})}}$ and obtain a finer T-mesh

$$\mathtt{refine}(\widehat{\mathcal{T}}_\bullet, \widehat{\mathcal{M}}_\bullet) := \widehat{\mathcal{T}}_\bullet \setminus \widehat{\mathcal{M}}_\bullet^{(j)} \cup \bigcup \big\{\mathtt{bisect}_{\mathrm{level}(\widehat{T})+1-\underline{\mathrm{level}(\widehat{T})}}(\widehat{T}) : \widehat{T} \in \widehat{\mathcal{M}}_\bullet^{(j)}\big\}, \tag{2.22}$$

where we recall from (2.4) that $\underline{\mathrm{level}(\widehat{T})} = \lfloor \mathrm{level}(\widehat{T})/d \rfloor d$.

Output: Refined mesh $\mathtt{refine}(\widehat{\mathcal{T}}_\bullet, \widehat{\mathcal{M}}_\bullet)$.

Remark 2.2. The additional bisection of neighbors (and their neighbors, etc.) of marked elements is required to ensure local quasi-uniformity (see (2.24)–(2.25) below) and *analysis-suitability* in the sense of (Beirão da Veiga et al., 2013; Morgenstern, 2016) for $d = 2, 3$, respectively. For $d = 2$, the latter is characterized by the assumption that horizontal *T-junction extensions* do not intersect vertical ones. In particular, this yields linear independence of the set of B-splines $\big\{\widehat{B}_{\bullet,z} : z \in \widehat{\mathcal{N}}_\bullet^{\mathrm{act}}\big\}$; see Section 2.3.

For any T-mesh $\widehat{\mathcal{T}}_\bullet$, we define $\mathtt{refine}(\widehat{\mathcal{T}}_\bullet)$ as the set of all T-meshes $\widehat{\mathcal{T}}_\circ$ such that there exist T-meshes $\widehat{\mathcal{T}}_{(0)}, \dots, \widehat{\mathcal{T}}_{(J)}$ and marked elements $\widehat{\mathcal{M}}_{(0)}, \dots, \widehat{\mathcal{M}}_{(J-1)}$ with $\widehat{\mathcal{T}}_\circ = \widehat{\mathcal{T}}_{(J)} = \mathtt{refine}(\widehat{\mathcal{T}}_{(J-1)}, \widehat{\mathcal{M}}_{(J-1)}), \dots, \widehat{\mathcal{T}}_{(1)} = \mathtt{refine}(\widehat{\mathcal{T}}_{(0)}, \widehat{\mathcal{M}}_{(0)})$, and $\widehat{\mathcal{T}}_{(0)} = \widehat{\mathcal{T}}_\bullet$; see Fig. 2.5 for some refined meshes. Here, we formally allow $J = 0$, i.e., $\widehat{\mathcal{T}}_\bullet \in \mathtt{refine}(\widehat{\mathcal{T}}_\bullet)$. Finally, we define the set of all *admissible T-meshes* as

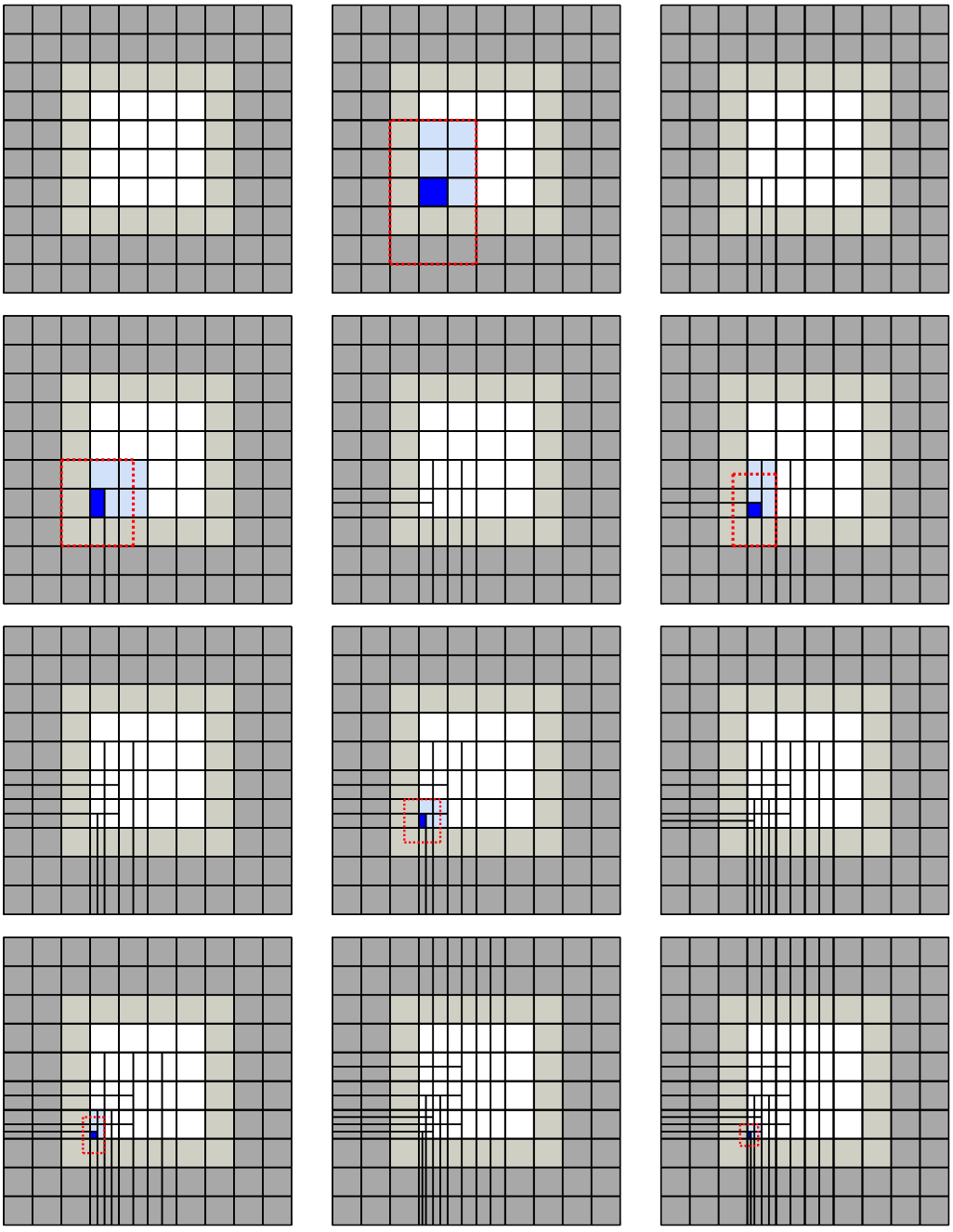

Fig. 2.5. An initial T-mesh $\widehat{\mathcal{T}}_0^{\mathrm{ext}}$ in 2D (top left) with $(p_1, p_2) = (3, 3)$ and its first five refinements towards the lower left corner of $\widehat{\Omega}$ are depicted. The sets $\widehat{\Omega}$, $\widehat{\Omega}^{\mathrm{act}}$, and $\widehat{\Omega}^{\mathrm{ext}}$ are highlighted in white, light gray, and dark gray, respectively. Every second picture shows the element (in blue) that is marked to obtain the next mesh. Its neighbors are shown in light blue. According to definition (2.18), the neighbors are all elements in $\overline{\widehat{\Omega}}$ with non-empty intersection with the rectangles indicated in red.

$$\widehat{\mathbb{T}} := \mathtt{refine}(\widehat{\mathcal{T}}_0). \tag{2.23}$$

For any admissible $\widehat{\mathcal{T}}_\bullet \in \widehat{\mathbb{T}}$, (Morgenstern and Peterseim, 2015, remark after Definition 2.4 and Lemma 2.14) proves for $d = 2$ that

$$|\mathrm{level}(\widehat{T}) - \mathrm{level}(\widehat{T}')| \leq 1 \quad \text{for all } \widehat{T}, \widehat{T}' \in \widehat{\mathcal{T}}_\bullet \text{ with } \widehat{T}' \in \mathbf{N}_\bullet(\widehat{T}), \tag{2.24}$$

as well as

$$\big\{\widehat{T}' \in \widehat{\mathcal{T}}_\bullet : \widehat{T} \cap \widehat{T}' \neq \emptyset\big\} \subseteq \mathbf{N}_\bullet(\widehat{T}) \quad \text{for all } \widehat{T} \in \widehat{\mathcal{T}}_\bullet. \tag{2.25}$$

Similarly, (Morgenstern, 2016, Lemma 3.5) proves (2.24)–(2.25) for $d = 3$.

Remark 2.3. As any element $\widehat{T} \in \widehat{\mathcal{T}}_\bullet \in \widehat{\mathbb{T}}$ of level k is essentially of size $2^{-k/2}$ if $d = 2$ and $2^{-k/3}$ if $d = 3$, the definition of $\mathbf{N}_\bullet(\widehat{T})$ and (2.24)–(2.25) yield that the number $\#\mathbf{N}_\bullet(\widehat{T})$ is uniformly bounded independently of the level. Moreover, for $d = 2$, (Morgenstern and Peterseim, 2015, remark after Definition 2.4) states that whenever $\widehat{T}$ is bisected (in direction $k + 1 - \underline{k}$), the resulting sons $\widehat{T}_1, \widehat{T}_2$ in the refined mesh $\widehat{\mathcal{T}}_\circ$ satisfy that $\mathbf{N}_\circ(\widehat{T}_i) \setminus \{\widehat{T}_1, \widehat{T}_2\} \subseteq \mathbf{N}_\bullet(\widehat{T}) \setminus \{\widehat{T}\}$. One elementarily sees that this inclusion also holds for $d = 3$. The latter two properties allow for an efficient implementation of Algorithm 2.1, where the neighbors of all elements in the current mesh are stored in a suitable data structure and updated after each bisection.

2.3. Basis of $\widehat{\mathcal{X}}_\bullet$

First, we emphasize that for general T-meshes $\widehat{\mathcal{T}}_\bullet$ as in Section 2.1, the set $\big\{\widehat{B}_{\bullet,z} : z \in \widehat{\mathcal{N}}_\bullet^{\mathrm{act}}\big\}$ is not necessarily a basis of the corresponding T-spline space $\widehat{\mathcal{Y}}_\bullet$ since it is not necessarily linearly independent; see (Buffa et al., 2010) for a counter example. According to (Beirão da Veiga et al., 2014, Proposition 7.4), a sufficient criterion for linear independence of a set of B-splines is dual-compatibility: We say that $\big\{\widehat{B}_{\bullet,z} : z \in \widehat{\mathcal{N}}_\bullet\big\}$ is *dual-compatible* if for all $z, z' \in \widehat{\mathcal{N}}_\bullet$ with $|\widehat{B}_{\bullet,z} \cap \widehat{B}_{\bullet,z'}| > 0$, the corresponding local knot vectors are at least in one direction aligned, i.e., there exists $i \in \{1, \dots, d\}$ such that $\widehat{\mathcal{K}}^{\mathrm{loc}}_{\bullet,i}(z)$ and $\widehat{\mathcal{K}}^{\mathrm{loc}}_{\bullet,i}(z')$ are both sub-vectors of one common sorted vector $\widehat{\mathcal{K}}$.

We stress that admissible meshes yield dual-compatible B-splines, where the local knot vectors are even aligned in at least two directions for $d = 3$, and thus linearly independent B-splines. Indeed, (Morgenstern and Peterseim, 2015, Theorem 3.6) and (Morgenstern, 2016, Theorem 5.3) prove analysis-suitability (see Remark 2.2) for $d = 2$ and $d = 3$, respectively. According to (Beirão da Veiga et al., 2014, Theorem 7.16) for $d = 2$ and (Morgenstern, 2016, Theorem 6.6) for $d = 3$, this implies the stated dual-compatibility. To be precise, (Morgenstern, 2016) defines the space of T-splines differently as the span of $\big\{\widehat{B}_{\bullet,z} : z \in \widehat{\mathcal{N}}_\bullet^{\mathrm{act}} \cap \overline{\widehat{\Omega}}\big\}$ and shows that this set is dual-compatible. The functions in this set are not only zero on the boundary $\partial\widehat{\Omega}$, but also some of their derivatives vanish there since the maximal multiplicity in the used local knot vectors is at most p_i in each direction; see, e.g., (de Boor, 2001, Section 6). Nevertheless, the proofs immediately generalize to our standard definition of T-splines. The following lemma provides a basis of $\widehat{\mathcal{X}}_\bullet$.

Lemma 2.4. *Let $\widehat{\mathcal{T}}_\bullet \in \widehat{\mathbb{T}}$ be an arbitrary admissible T-mesh in the parameter domain $\widehat{\Omega}$. Then, $\big\{\widehat{B}_{\bullet,z} : z \in \widehat{\mathcal{N}}_\bullet^{\mathrm{act}} \setminus \partial\widehat{\Omega}^{\mathrm{act}}\big\}$ is a basis of $\widehat{\mathcal{X}}_\bullet$.*

Proof. Since we already know that the set $\big\{\widehat{B}_{\bullet,z} : z \in \widehat{\mathcal{N}}_\bullet^{\mathrm{act}} \setminus \partial\widehat{\Omega}^{\mathrm{act}}\big\}$ is linearly independent, we only have to show that it generates $\widehat{\mathcal{X}}_\bullet$.

Step 1: We recall that the one-dimensional B-spline $\widehat{B}(\cdot|x_0, \dots, x_{p+1})$ induced by a sorted knot vector $(x_0, \dots, x_{p+1}) \in \mathbb{R}^{p+2}$ is positive on the interval (x_0, x_{p+1}). It does not vanish at x_0 if and only if $x_0 = \cdots = x_p$, and it does not vanish at x_{p+1} if and only if $x_1 = \cdots = x_{p+1}$. In particular, for all $z \in \widehat{\mathcal{N}}_\bullet^{\mathrm{act}}$, this and the tensor-product structure of $\widehat{B}_{\bullet,z}$ yield that $\widehat{B}_{\bullet,z}|_{\partial\widehat{\Omega}} \neq 0$ if and only if $z \in \partial\widehat{\Omega}^{\mathrm{act}}$; see also Fig. 2.3. This shows that

$$\operatorname{span}\big\{\widehat{B}_{\bullet,z} : z \in \widehat{\mathcal{N}}_\bullet^{\mathrm{act}} \setminus \partial\widehat{\Omega}^{\mathrm{act}}\big\} \subseteq \widehat{\mathcal{X}}_\bullet. \tag{2.26}$$

Step 2: To see the other inclusion, let $\widehat{V}_\bullet \in \widehat{\mathcal{X}}_\bullet$. Then, there exists a representation of the form $\widehat{V}_\bullet = \sum_{z \in \widehat{\mathcal{N}}_\bullet^{\mathrm{act}}} c_z \widehat{B}_{\bullet,z}$. Let $\widehat{E}$ be an arbitrary facet of the boundary $\partial\widehat{\Omega}$ and $\widehat{E}^{\mathrm{act}}$ its extension onto $\partial\widehat{\Omega}^{\mathrm{act}}$, i.e.,

$$\widehat{E} := \prod_{j=1}^{i-1} [0, N_j] \times \{\widehat{e}\} \times \prod_{j=i+1}^{d} [0, N_j],$$

$$\widehat{E}^{\mathrm{act}} := \prod_{j=1}^{i-1} [-(p_j - 1)/2, N_j + (p_j - 1)/2] \times \{\widehat{e}^{\mathrm{act}}\} \times \prod_{j=i+1}^{d} [-(p_j - 1)/2, N_j + (p_j - 1)/2],$$

with $i \in \{1, \dots, d\}$, $\widehat{e} := 0$ and $\widehat{e}^{\mathrm{act}} := -(p_i - 1)/2$, or $\widehat{e} := N_i$ and $\widehat{e}^{\mathrm{act}} := N_i + (p_i - 1)/2$. Restricting onto $\widehat{E}$ and using the argument from Step 1, we derive that

$$0 = \widehat{V}_\bullet|_{\widehat{E}} = \sum_{z \in \widehat{\mathcal{N}}_\bullet^{\mathrm{act}}} c_z \widehat{B}_{\bullet,z}|_{\widehat{E}} = \sum_{z \in \widehat{\mathcal{N}}_\bullet^{\mathrm{act}} \cap \widehat{E}^{\mathrm{act}}} c_z \widehat{B}_{\bullet,z}|_{\widehat{E}}.$$

For $d = 2$, the set $\big\{\widehat{B}_{\bullet,z}|_{\widehat{E}} : z \in \widehat{\mathcal{N}}_\bullet^{\mathrm{act}} \cap \widehat{E}^{\mathrm{act}}\big\}$ coincides (up to the domain of definition) with the set of $(d-1)$-dimensional B-splines corresponding to the global knot vector $\widehat{\mathcal{K}}^{\mathrm{gl}}_{\bullet,i}((0,0))$ if $\widehat{e} = 0$ and $\widehat{\mathcal{K}}^{\mathrm{gl}}_{\bullet,i}((N_1, N_2))$ if $\widehat{e} = N_i$; see, e.g., (de Boor, 2001,

Section 2) for a precise definition of the set of B-splines associated to some global knot vector. It is well-known that these functions are linearly independent, wherefore we derive that $c_z = 0$ for the corresponding coefficients.

For $d = 3$, the set $\{\widehat{B}_{\bullet,z}|_{\widehat{E}} : z \in \widehat{\mathcal{N}}_\bullet^{\mathrm{act}} \cap \widehat{E}^{\mathrm{act}}\}$ coincides (up to the domain of definition) with the set of $(d-1)$-dimensional B-splines corresponding to the $(d-1)$-dimensional T-mesh

$$\widehat{\mathcal{T}}_\bullet^{\mathrm{ext}}|_{\widehat{E}^{\mathrm{ext}}} := \Big\{ \prod_{\substack{j=1\\ j\neq i}}^{i-1} [a_j, b_j] : \prod_{j=1}^{d} [a_j, b_j] \in \widehat{\mathcal{T}}_\bullet^{\mathrm{ext}} \wedge a_i = \widehat{e} \Big\}. \tag{2.27}$$

We have already mentioned that (Morgenstern, 2016, Theorem 5.3 and Theorem 6.6) shows that the local knot vectors of the B-spline basis of $\widehat{\mathcal{Y}}_\bullet$ are even aligned in at least two directions. In particular, the knot vectors of the B-splines corresponding to the mesh $\widehat{\mathcal{T}}_\bullet^{\mathrm{ext}}|_{\widehat{E}^{\mathrm{ext}}}$ are aligned in at least one direction. This yields dual-compatibility and thus linear independence of these B-splines, which concludes that $c_z = 0$ for the corresponding coefficients. Since $\partial\widehat{\Omega}^{\mathrm{act}}$ is the union of all its facets and $\widehat{E}$ was arbitrary, this concludes that $c_z = 0$ for all $z \in \widehat{\mathcal{N}}_\bullet^{\mathrm{act}} \cap \partial\widehat{\Omega}^{\mathrm{act}}$ and thus the other inclusion in (2.26). □

Finally, we study the support of the basis functions of $\widehat{\mathcal{Y}}_\bullet$ (and thus of $\widehat{\mathcal{X}}_\bullet$). To this end, we define for $\widehat{\mathcal{T}}_\bullet \in \widehat{\mathbb{T}}$ and $\widehat{\omega} \subseteq \overline{\widehat{\Omega}}$, the patches of order $k \in \mathbb{N}$ inductively by

$$\pi_\bullet^0(\widehat{\omega}) := \widehat{\omega}, \quad \pi_\bullet^k(\widehat{\omega}) := \bigcup \{\widehat{T} \in \widehat{\mathcal{T}}_\bullet : \widehat{T} \cap \pi_\bullet^{k-1}(\widehat{\omega}) \neq \emptyset\}. \tag{2.28}$$

Lemma 2.5. *Let $\widehat{\mathcal{T}}_\bullet \in \widehat{\mathbb{T}}$, $\widehat{T} \in \widehat{\mathcal{T}}_\bullet$, and $z \in \widehat{\mathcal{N}}_\bullet^{\mathrm{act}}$ with $|\widehat{T} \cap \mathrm{supp}(\widehat{B}_{\bullet,z})| > 0$. Then, there exists a uniform $k_{\mathrm{supp}} \in \mathbb{N}_0$ such that $\mathrm{supp}(\widehat{B}_{\bullet,z}) \subseteq \pi_\bullet^{k_{\mathrm{supp}}}(\widehat{T})$. Moreover, there exist only k_{supp} nodes $z' \in \widehat{\mathcal{N}}_\bullet^{\mathrm{act}}$ such that $|\widehat{T} \cap \mathrm{supp}(\widehat{B}_{\bullet,z'})| > 0$. The constant k_{supp} depends only on d and $(p_1, \dots, p_d)$.*

Proof. We prove the assertion in two steps.

Step 1: We prove the first assertion. Without loss of generality, we can assume that $z \in \overline{\widehat{\Omega}}$, since otherwise there exists $z'' \in \widehat{\mathcal{N}}_\bullet^{\mathrm{act}} \cap \overline{\widehat{\Omega}}$ (namely the projection of z into $\overline{\widehat{\Omega}}$) such that $\mathrm{supp}(\widehat{B}_{\bullet,z}) \subseteq \mathrm{supp}(\widehat{B}_{\bullet,z''})$ (see (2.14)) and the assertion for z'' yields that $\mathrm{supp}(\widehat{B}_{\bullet,z}) \subseteq \pi_\bullet^{k_{\mathrm{supp}}}(\widehat{T})$. Obviously, the support of $\widehat{B}_{\bullet,z}$ can be covered by elements in $\widehat{\mathcal{T}}_\bullet$, i.e., $\mathrm{supp}(\widehat{B}_{\bullet,z}) \subseteq \bigcup \widehat{\mathcal{T}}_\bullet = \overline{\widehat{\Omega}}$. We show that $|\widehat{T}| \simeq |\mathrm{supp}(\widehat{B}_{\bullet,z})|$. Let $\widehat{T}_z \in \widehat{\mathcal{T}}_\bullet$ with $z \in \widehat{T}_z$ and thus $\widehat{T}_z \subseteq \mathrm{supp}(\widehat{B}_{\bullet,z})$. Then, (2.24)–(2.25) and the definition of $\widehat{B}_{\bullet,z}$ show that

$$|\widehat{T}_z| \simeq |\mathrm{supp}(\widehat{B}_{\bullet,z})|. \tag{2.29}$$

Now, let $z_{\widehat{T}} \in \widehat{\mathcal{N}}_\bullet^{\mathrm{act}}$ with $z_{\widehat{T}} \in \widehat{T}$ and thus $\widehat{T} \subseteq \mathrm{supp}(\widehat{B}_{\bullet,z_{\widehat{T}}})$. Then, we have that $|\mathrm{supp}(\widehat{B}_{\bullet,z}) \cap \mathrm{supp}(\widehat{B}_{\bullet,z_{\widehat{T}}})| > 0$. Since $\widehat{\mathcal{T}}_\bullet$ yields dual-compatible B-splines, the knot lines of $\widehat{B}_{\bullet,z}$ and $\widehat{B}_{\bullet,z_{\widehat{T}}}$ are aligned in one direction. Moreover, due to (2.24)–(2.25), the difference between consecutive knot lines is equivalent to $2^{-\mathrm{level}(\widehat{T}_z)/2}$ and $2^{-\mathrm{level}(\widehat{T})/2}$, respectively. Thus, we obtain that $\mathrm{level}(\widehat{T}_z) \simeq \mathrm{level}(\widehat{T})$ and $|\widehat{T}_z| \simeq |\widehat{T}|$. In combination with (2.29), we derive that $|\widehat{T}| \simeq |\mathrm{supp}(\widehat{B}_{\bullet,z})|$. Since $\widehat{T}$ is arbitrary and $\mathrm{supp}(\widehat{B}_{\bullet,z})$ is connected, this yields the existence of $k'_{\mathrm{supp}} \in \mathbb{N}_0$ with $\mathrm{supp}(\widehat{B}_{\bullet,z}) \subseteq \pi_\bullet^{k'_{\mathrm{supp}}}(\widehat{T})$.

Step 2: We prove the second assertion. First, let $z' \in \widehat{\mathcal{N}}_\bullet^{\mathrm{act}} \cap \overline{\widehat{\Omega}}$. Then, Step 1 gives that $z' \in \mathrm{supp}(\widehat{B}_{\bullet,z'}) \subseteq \pi_\bullet^{k_{\mathrm{supp}}}(\widehat{T})$. Therefore, we see that the number of such z' is bounded by $\#(\widehat{\mathcal{N}}_\bullet^{\mathrm{act}} \cap \overline{\widehat{\Omega}} \cap \pi_\bullet^{k_{\mathrm{supp}}}(\widehat{T}))$. If $z' \in \widehat{\mathcal{N}}_\bullet^{\mathrm{act}} \setminus \overline{\widehat{\Omega}}$, there exists $z'' \in \widehat{\mathcal{N}}_\bullet^{\mathrm{act}} \cap \overline{\widehat{\Omega}}$ (namely the projection of z' into $\overline{\widehat{\Omega}}$) such that $\mathrm{supp}(\widehat{B}_{\bullet,z'}) \subseteq \mathrm{supp}(\widehat{B}_{\bullet,z''})$ and thus $|\mathrm{supp}(\widehat{T} \cap \widehat{B}_{\bullet,z''})| > 0$. On the other hand, for given $z'' \in \widehat{\mathcal{N}}_\bullet^{\mathrm{act}} \cap \overline{\widehat{\Omega}}$, the number of $z' \in \widehat{\mathcal{N}}_\bullet^{\mathrm{act}} \setminus \overline{\widehat{\Omega}}$ with $\mathrm{supp}(\widehat{B}_{\bullet,z'}) \subseteq \mathrm{supp}(\widehat{B}_{\bullet,z''})$ is uniformly bounded by some constant $C > 0$ depending only on d and $(p_1, \dots, p_d)$; see also Fig. 2.3. Altogether, we see that the number of $z' \in \widehat{\mathcal{N}}_\bullet^{\mathrm{act}}$ with $|\mathrm{supp}(\widehat{B}_{\bullet,z'}) \cap \widehat{T}| > 0$ is bounded by $(1+C)\#(\widehat{\mathcal{N}}_\bullet^{\mathrm{act}} \cap \overline{\widehat{\Omega}} \cap \pi_\bullet^{k_{\mathrm{supp}}}(\widehat{T}))$. Due to (2.24)–(2.25), this term is bounded by some uniform constant $k''_{\mathrm{supp}} \in \mathbb{N}_0$. Finally, we set $k_{\mathrm{supp}} := \max(k'_{\mathrm{supp}}, k''_{\mathrm{supp}})$. □

2.4. T-meshes and splines in the physical domain Ω

To transform the definitions in the parameter domain $\widehat{\Omega}$ to the physical domain Ω, we assume as in (Gantner et al., 2017, Section 3.6) that we are given a bi-Lipschitz continuous piecewise C^2 parametrization

$$\gamma : \overline{\widehat{\Omega}} \to \overline{\Omega} \quad \text{with} \quad \gamma \in W^{1,\infty}(\widehat{\Omega}) \cap C^2(\widehat{\mathcal{T}}_0) \quad \text{and} \quad \gamma^{-1} \in W^{1,\infty}(\Omega) \cap C^2(\mathcal{T}_0), \tag{2.30}$$

where $C^2(\widehat{\mathcal{T}}_0) := \{v : \overline{\widehat{\Omega}} \to \mathbb{R} : v|_{\widehat{T}} \in C^2(\widehat{T}) \text{ for all } \widehat{T} \in \widehat{\mathcal{T}}_0\}$ and $C^2(\mathcal{T}_0) := \{v : \overline{\Omega} \to \mathbb{R} : v|_T \in C^2(T) \text{ for all } T \in \mathcal{T}_0\}$. Consequently, there exists $C_\gamma > 0$ such that for all $i, j, k \in \{1, \dots, d\}$

$$\begin{aligned} \left\| \frac{\partial}{\partial t_j} \gamma_i \right\|_{L^\infty(\widehat{\Omega})} \le C_\gamma, \quad \left\| \frac{\partial}{\partial x_j} (\gamma^{-1})_i \right\|_{L^\infty(\Omega)} \le C_\gamma, \\ \left\| \frac{\partial^2}{\partial t_j \partial t_k} \gamma_i \right\|_{L^\infty(\widehat{\Omega})} \le C_\gamma, \quad \left\| \frac{\partial^2}{\partial x_j \partial x_k} (\gamma^{-1})_i \right\|_{L^\infty(\Omega)} \le C_\gamma, \end{aligned} \tag{2.31}$$

where γ_i resp. $(\gamma^{-1})_i$ denotes the i-th component of γ resp. γ^{-1} and any second derivative is meant $\mathcal{T}_0$-elementwise. All previous definitions can now also be made in the physical domain, just by pulling them from the parameter domain via the diffeomorphism γ. For these definitions, we drop the symbol $\widehat{\cdot}$. Given $\widehat{\mathcal{T}}_\bullet \in \widehat{\mathbb{T}}$, the corresponding mesh in the physical domain reads $\mathcal{T}_\bullet := \{\gamma(\widehat{T}) : \widehat{T} \in \widehat{\mathcal{T}}_\bullet\}$. In particular, we have that $\mathcal{T}_0 = \{\gamma(\widehat{T}) : \widehat{T} \in \widehat{\mathcal{T}}_0\}$. Moreover, let $\mathbb{T} := \{\mathcal{T}_\bullet : \widehat{\mathcal{T}}_\bullet \in \widehat{\mathbb{T}}\}$ be the set of admissible meshes in the physical domain. If now $\mathcal{M}_\bullet \subseteq \mathcal{T}_\bullet$ with $\mathcal{T}_\bullet \in \mathbb{T}$, we abbreviate $\widehat{\mathcal{M}}_\bullet := \{\gamma^{-1}(T) : T \in \mathcal{M}_\bullet\}$ and define $\texttt{refine}(\mathcal{T}_\bullet, \mathcal{M}_\bullet) := \{\gamma(\widehat{T}) : \widehat{T} \in \texttt{refine}(\widehat{\mathcal{T}}_\bullet, \widehat{\mathcal{M}}_\bullet)\}$. For $\mathcal{T}_\bullet \in \mathbb{T}$, let $\mathcal{Y}_\bullet := \{\widehat{V}_\bullet \circ \gamma^{-1} : \widehat{V}_\bullet \in \widehat{\mathcal{Y}}_\bullet\}$ be the corresponding space of T-splines, and $\mathcal{X}_\bullet := \{\widehat{V}_\bullet \circ \gamma^{-1} : \widehat{V}_\bullet \in \widehat{\mathcal{X}}_\bullet\}$ the corresponding space of T-splines which vanish on the boundary. By regularity of γ, we especially obtain that

$$\mathcal{X}_\bullet \subset \{v \in H^1_0(\Omega) : v|_T \in H^2(T) \text{ for all } T \in \mathcal{T}_\bullet\}. \tag{2.32}$$

Let $U_\bullet \in \mathcal{X}_\bullet$ be the corresponding Galerkin approximation to the solution $u \in H^1_0(\Omega)$, i.e.,

$$\langle U_\bullet, V_\bullet \rangle_{\mathcal{L}} = \int_\Omega f V_\bullet - \boldsymbol{f} \cdot \nabla V_\bullet \, dx \quad \text{for all } V_\bullet \in \mathcal{X}_\bullet. \tag{2.33}$$

We note the Galerkin orthogonality

$$\langle u - U_\bullet, V_\bullet \rangle_{\mathcal{L}} = 0 \quad \text{for all } V_\bullet \in \mathcal{X}_\bullet \tag{2.34}$$

as well as the resulting Céa-type quasi-optimality

$$\|u - U_\bullet\|_{H^1(\Omega)} \le C_{\text{Céa}} \min_{V_\bullet \in \mathcal{X}_\bullet} \|u - V_\bullet\|_{H^1(\Omega)} \quad \text{with} \quad C_{\text{Céa}} := \frac{\|\boldsymbol{A}\|_{L^\infty(\Omega)} + \|\boldsymbol{b}\|_{L^\infty(\Omega)} + \|c\|_{L^\infty(\Omega)}}{C_{\text{ell}}}. \tag{2.35}$$

2.5. Error estimator

Let $\mathcal{T}_\bullet \in \mathbb{T}$ and $T_1 \in \mathcal{T}_\bullet$. For almost every $x \in \partial T_1 \cap \Omega$, there exists a unique element $T_2 \in \mathcal{T}_\bullet$ with $x \in T_1 \cap T_2$. We denote the corresponding outer normal vectors by ν_1 and ν_2 and define the normal jump as

$$[(\boldsymbol{A}\nabla U_\bullet + \boldsymbol{f}) \cdot \nu](x) = (\boldsymbol{A}\nabla U_\bullet + \boldsymbol{f})|_{T_1}(x) \cdot \nu_1(x) + (\boldsymbol{A}\nabla U_\bullet + \boldsymbol{f})|_{T'}(x) \cdot \nu_2(x). \tag{2.36}$$

With this definition, we employ the residual *a posteriori* error estimator

$$\eta_\bullet := \eta_\bullet(\mathcal{T}_\bullet) \quad \text{with} \quad \eta_\bullet(\mathcal{S}_\bullet)^2 := \sum_{T \in \mathcal{S}_\bullet} \eta_\bullet(T)^2 \text{ for all } \mathcal{S}_\bullet \subseteq \mathcal{T}_\bullet, \tag{2.37a}$$

where, for all $T \in \mathcal{T}_\bullet$, the local refinement indicators read

$$\eta_\bullet(T)^2 := |T|^{2/d} \|f + \operatorname{div}(\boldsymbol{A}\nabla U_\bullet + \boldsymbol{f}) - \boldsymbol{b} \cdot \nabla U_\bullet - c U_\bullet\|^2_{L^2(T)} + |T|^{1/d} \|[(\boldsymbol{A}\nabla U_\bullet + \boldsymbol{f}) \cdot \nu]\|^2_{L^2(\partial T \cap \Omega)}. \tag{2.37b}$$

We refer, e.g., to the monographs (Ainsworth and Oden, 2000; Verfürth, 2013) for the analysis of the residual *a posteriori* error estimator (2.37) in the frame of standard FEM with piecewise polynomials of fixed order.

Remark 2.6. If $\mathcal{X}_\bullet \subset C^1(\Omega)$, then the jump contributions in (2.37) vanish and $\eta_\bullet(T)$ consists only of the volume residual.

2.6. Adaptive algorithm

We consider the common formulation of an adaptive mesh-refining algorithm; see, e.g., Algorithm 2.2 of (Carstensen et al., 2014).

Algorithm 2.7. Input: Adaptivity parameter $0 < \theta \le 1$ and marking constant $C_{\text{min}} \ge 1$.
Loop: For each $\ell = 0, 1, 2, \dots$, iterate the following steps (i)–(iv):

(i) Compute Galerkin approximation $U_\ell \in \mathcal{X}_\ell$.
(ii) Compute refinement indicators $\eta_\ell(T)$ for all elements $T \in \mathcal{T}_\ell$.
(iii) Determine a set of marked elements $\mathcal{M}_\ell \subseteq \mathcal{T}_\ell$ with $\theta\, \eta_\ell^2 \le \eta_\ell(\mathcal{M}_\ell)^2$ which has up to the multiplicative constant C_{min} minimal cardinality.
(iv) Generate refined mesh $\mathcal{T}_{\ell+1} := \texttt{refine}(\mathcal{T}_\ell, \mathcal{M}_\ell)$.

Output: Sequence of successively refined meshes $\mathcal{T}_\ell$ and corresponding Galerkin approximations U_ℓ with error estimators η_ℓ for all $\ell \in \mathbb{N}_0$.

Remark 2.8. For the sake of simplicity, we assume that U_ℓ is computed exactly. However, according to (Carstensen et al., 2014, Section 7), the forthcoming optimality analysis remains valid if U_ℓ is replaced by an approximation $\widetilde{U}_\ell \in \mathcal{X}_\ell$ such that

$$\|U_\ell - \widetilde{U}_\ell\|_{\mathcal{L}} \le \vartheta\, \eta_\ell(\widetilde{U}_\ell) \tag{2.38}$$

with the energy norm $\|\cdot\|_{\mathcal{L}}^2 := \langle\cdot\,,\cdot\rangle_{\mathcal{L}}$, the error estimator $\eta_\ell(\widetilde{U}_\ell)$ defined analogously as in (2.37), and a sufficiently small but fixed adaptivity parameter $0 < \vartheta < 1$. In practice, (2.38) can be efficiently realized if one preconditions the arising linear system appropriately and then solves it iteratively; see (Führer et al., 2019) in case of the boundary element method. Assuming $\mathcal{L}$ to be symmetric, i.e., $\boldsymbol{b} = 0$, one employs PCG-iterations (Golub and van Loan, 2012) starting from $\widetilde{U}_\ell^0 := \widetilde{U}_{\ell-1}$ with $\widetilde{U}_{-1} := 0$ until

$$\|\widetilde{U}_\ell^j - \widetilde{U}_\ell^{j-1}\|_{\mathcal{L}} \le \vartheta'\, \eta_\ell(\widetilde{U}_\ell^j), \tag{2.39}$$

and $\widetilde{U}_\ell$ is defined as the final PCG-iterate $\widetilde{U}_\ell^j$. For analysis-suitable T-splines and the Poisson model problem, appropriate preconditioners have recently been developed in (Cho and Vázquez, 2020). At least for the Poisson model problem, this gives rise to an extended version of Algorithm 2.7 which does not only converge at optimal rate with respect to the number of mesh elements, but also with respect to the overall computational cost; see (Gantner et al., 2020b) for a recent development.

2.7. Data oscillations

We fix polynomial orders $(q_1, \dots, q_d)$ and define for $\mathcal{T}_\bullet \in \mathbb{T}$ the space of transformed polynomials

$$\mathcal{P}(\Omega) := \big\{ \widehat{V} \circ \gamma : \widehat{V} \text{ is a tensor-polynomial of order } (q_1, \dots, q_d) \big\}. \tag{2.40}$$

Remark 2.9. In order to obtain higher-order oscillations, the natural choice of the polynomial orders is $q_i \ge 2p_i - 1$ for $i \in \{1 \dots, d\}$; see, e.g., (Nochetto and Veeser, 2012, Section 3.1). If $\mathcal{X}_\bullet \subset C^1(\Omega)$, it is sufficient to choose $q_i \ge 2p_i - 2$; see Remark 2.10.

Let $\mathcal{T}_\bullet \in \mathbb{T}$. For $T \in \mathcal{T}_\bullet$, we define the L^2-orthogonal projection $P_{\bullet,T} : L^2(T) \to \big\{W|_T : W \in \mathcal{P}(\Omega)\big\}$. For an interior edge $E \in \mathcal{E}_{\bullet,T} := \big\{T \cap T' : T' \in \mathcal{T}_\bullet \wedge \dim(T \cap T') = d-1\big\}$, we define the L^2-orthogonal projection $P_{\bullet,E} : L^2(E) \to \big\{W|_E : W \in \mathcal{P}(\Omega)\big\}$. Note that $\bigcup \mathcal{E}_{\bullet,T} = \overline{\partial T \cap \Omega}$. For $V_\bullet \in \mathcal{X}_\bullet$, we define the corresponding oscillations

$$\operatorname{osc}_\bullet(V_\bullet) := \operatorname{osc}_\bullet(V_\bullet, \mathcal{T}_\bullet) \quad \text{with} \quad \operatorname{osc}_\bullet(V_\bullet, \mathcal{S}_\bullet)^2 := \sum_{T \in \mathcal{S}_\bullet} \operatorname{osc}_\bullet(V_\bullet, T)^2 \text{ for all } \mathcal{S}_\bullet \subseteq \mathcal{T}_\bullet, \tag{2.41a}$$

where, for all $T \in \mathcal{T}_\bullet$, the local oscillations read

$$\begin{aligned} \operatorname{osc}_\bullet(V_\bullet, T)^2 := {} & |T|^{2/d} \|(1 - P_{\bullet,T})(f + \operatorname{div}(\boldsymbol{A}\nabla V_\bullet + \boldsymbol{f}) - \boldsymbol{b}\cdot\nabla V_\bullet - cV_\bullet)\|_{L^2(T)}^2 \\ & + \sum_{E \in \mathcal{E}_{\bullet,T}} |T|^{1/d} \|(1 - P_{\bullet,E})[(\boldsymbol{A}\nabla V_\bullet + \boldsymbol{f})\cdot\nu]\|_{L^2(E)}^2. \end{aligned} \tag{2.41b}$$

We refer, e.g., to (Nochetto and Veeser, 2012) for the analysis of oscillations in the frame of standard FEM with piecewise polynomials of fixed order.

Remark 2.10. If $\mathcal{X}_\bullet \subset C^1(\Omega)$, then the jump contributions in (2.41) vanish and $\operatorname{osc}_\bullet(V_\bullet, T)$ consists only of the volume oscillations.

2.8. Main result

Let

$$\mathbb{T}(N) := \big\{\mathcal{T}_\bullet \in \mathbb{T} : \#\mathcal{T}_\bullet - \#\mathcal{T}_0 \le N\big\} \quad \text{for all } N \in \mathbb{N}_0. \tag{2.42}$$

For all $s > 0$, define

$$\|u\|_{\mathbb{A}_s} := \sup_{N \in \mathbb{N}_0} \min_{\mathcal{T}_\bullet \in \mathbb{T}(N)} (N+1)^s\, \eta_\bullet \in [0, \infty] \tag{2.43}$$

and

$$\|u\|_{\mathbb{B}_s} := \sup_{N\in\mathbb{N}_0} \Big(\min_{\mathcal{T}_\bullet\in\mathbb{T}(N)} (N+1)^s \inf_{V_\bullet\in\mathcal{X}_\bullet} \big(\|u-V_\bullet\|_{H^1(\Omega)} + \operatorname{osc}_\bullet(V_\bullet)\big)\Big) \in [0,\infty]. \tag{2.44}$$

By definition, $\|u\|_{\mathbb{A}_s} < \infty$ (or $\|u\|_{\mathbb{B}_s} < \infty$) implies that the error estimator $\eta_\bullet$ (or the total error) on the optimal meshes $\mathcal{T}_\bullet$ decays at least with rate $\mathcal{O}\big((\#\mathcal{T}_\bullet)^{-s}\big)$. The following main theorem states that Algorithm 2.7 reaches each possible rate $s > 0$. The proof builds upon the analysis of (Gantner et al., 2017) and is given in Section 3. Generalizations are found in Section 4.

Theorem 2.11. *The following four assertions* (i)–(iv) *hold:*

(i) *The residual error estimator* (2.37) *satisfies reliability, i.e., there exists a constant* $C_{\mathrm{rel}} > 0$ *such that*

$$\|u-U_\bullet\|_{H^1(\Omega)} + \operatorname{osc}_\bullet \le C_{\mathrm{rel}}\eta_\bullet \quad \text{for all } \mathcal{T}_\bullet \in \mathbb{T}. \tag{2.45}$$

(ii) *The residual error estimator satisfies efficiency, i.e., there exists a constant* $C_{\mathrm{eff}} > 0$ *such that*

$$C_{\mathrm{eff}}^{-1}\eta_\bullet \le \inf_{V_\bullet\in\mathcal{X}_\bullet} \big(\|u-V_\bullet\|_{H^1(\Omega)} + \operatorname{osc}_\bullet(V_\bullet)\big). \tag{2.46}$$

(iii) *For arbitrary* $0 < \theta \le 1$ *and* $C_{\mathrm{min}} \ge 1$, *there exist constants* $C_{\mathrm{lin}} > 0$ *and* $0 < q_{\mathrm{lin}} < 1$ *such that the estimator sequence of Algorithm 2.7 guarantees linear convergence in the sense of*

$$\eta_{\ell+j}^2 \le C_{\mathrm{lin}} q_{\mathrm{lin}}^j \eta_\ell^2 \quad \text{for all } j,\ell \in \mathbb{N}_0. \tag{2.47}$$

(iv) *There exists a constant* $0 < \theta_{\mathrm{opt}} \le 1$ *such that for all* $0 < \theta < \theta_{\mathrm{opt}}$, *all* $C_{\mathrm{min}} \ge 1$, *and all* $s > 0$, *there exist constants* $c_{\mathrm{opt}}, C_{\mathrm{opt}} > 0$ *such that*

$$c_{\mathrm{opt}}\|u\|_{\mathbb{A}_s} \le \sup_{\ell\in\mathbb{N}_0} (\#\mathcal{T}_\ell - \#\mathcal{T}_0 + 1)^s \eta_\ell \le C_{\mathrm{opt}}\|u\|_{\mathbb{A}_s}, \tag{2.48}$$

i.e., the estimator sequence will decay with each possible rate $s > 0$.

The constants $C_{\mathrm{rel}}, C_{\mathrm{eff}}, C_{\mathrm{lin}}, q_{\mathrm{lin}}, \theta_{\mathrm{opt}}$, *and* C_{opt} *depend only on* d, *the coefficients of the differential operator* $\mathcal{L}$, $\operatorname{diam}(\Omega)$, C_γ, *and* $(p_1,\dots,p_d)$, *where* $C_{\mathrm{lin}}, q_{\mathrm{lin}}$ *depend additionally on* θ *and the sequence* $(U_\ell)_{\ell\in\mathbb{N}_0}$, *and* C_{opt} *depends furthermore on* C_{min}, *and* $s > 0$. *Finally,* c_{opt} *depends only on* C_{son}, $\#\mathcal{T}_0$, *and* s.

Remark 2.12. In particular, it holds that

$$C_{\mathrm{eff}}^{-1}\|u\|_{\mathbb{A}_s} \le \|u\|_{\mathbb{B}_s} \le C_{\mathrm{rel}}\|u\|_{\mathbb{A}_s} \quad \text{for all } s > 0. \tag{2.49}$$

If one applies continuous piecewise polynomials of degree p on a triangulation of some polygonal or polyhedral domain Ω as ansatz space, (Gaspoz and Morin, 2008) proves that $\|u\|_{\mathbb{B}_{p/d}} < \infty$. The proof requires that u allows for a certain decomposition and that the oscillations are of higher order; see Remark 2.9. In our case, $\|u\|_{\mathbb{A}_s} \simeq \|u\|_{\mathbb{B}_s}$ depends besides the polynomial degrees $(p_1,\dots,p_d)$ also on the (piecewise) smoothness of the parametrization γ. In practice, γ is usually piecewise C^∞. Given this additional regularity of γ, one might expect that the result of (Gaspoz and Morin, 2008) can be generalized such that $\|u\|_{\mathbb{A}_s}, \|u\|_{\mathbb{B}_s} < \infty$ for $s = \min_{i=1,\dots,d} p_i/d$. However, the proof goes beyond the scope of the present work and is left to future research.

Remark 2.13. Note that almost minimal cardinality of $\mathcal{M}_\ell$ in Algorithm 2.7 (iii) is only required to prove optimal convergence behavior (2.48), while linear convergence (2.47) formally allows $C_{\mathrm{min}} = \infty$, i.e., it suffices that $\mathcal{M}_\ell$ satisfies the Dörfler marking criterion. We refer to (Carstensen et al., 2014, Section 4.3–4.4) for details.

Remark 2.14. (a) If the bilinear form $\langle\cdot\,,\cdot\rangle_{\mathcal{L}}$ is symmetric, C_{lin}, q_{lin} as well as c_{opt}, C_{opt} are independent of $(U_\ell)_{\ell\in\mathbb{N}_0}$; see (Gantner et al., 2017, Remark 4.1).

(b) If the bilinear form $\langle\cdot\,,\cdot\rangle_{\mathcal{L}}$ is non-symmetric, there exists an index $\ell_0 \in \mathbb{N}_0$ such that the constants C_{lin}, q_{lin} as well as c_{opt}, C_{opt} are independent of $(U_\ell)_{\ell\in\mathbb{N}_0}$ if (2.47)–(2.48) are formulated only for $\ell \ge \ell_0$. We refer to the recent work (Bespalov et al., 2017, Theorem 19).

Remark 2.15. Let $h_\ell := \max_{T\in\mathcal{T}_\ell} |T|^{1/d}$ be the maximal mesh-width. Then, $h_\ell \to 0$ as $\ell\to\infty$, ensures that $\mathcal{X}_\infty := \overline{\bigcup_{\ell\in\mathbb{N}_0}\mathcal{X}_\ell} = H_0^1(\Omega)$; see (Gantner et al., 2017, Remark 2.7) for the elementary proof. We note that the latter observation allows to follow the ideas of (Bespalov et al., 2017) to show that the adaptive algorithm yields optimal convergence even if the bilinear form $\langle\cdot\,,\cdot\rangle_{\mathcal{L}}$ is only elliptic up to some compact perturbation provided that the continuous problem is well-posed. This includes, e.g., adaptive FEM for the Helmhotz equation; see (Bespalov et al., 2017).

3. Proof of Theorem 2.11

In (Gantner et al., 2017, Section 2), we have identified abstract properties of the underlying meshes, the mesh-refinement, the finite element spaces, and the oscillations which imply Theorem 2.11; see (Gantner, 2017, Section 4.2–4.3) for more details. We mention that (Gantner et al., 2017; Gantner, 2017) actually only treat the case $\boldsymbol{f} = 0$, but the corresponding proofs immediately extend to more general $\boldsymbol{f}$ as in Section 1.2. In the remainder of this section, we recapitulate these properties and verify them for our considered T-spline setting. For their formulation, we define for $\mathcal{T}_\bullet \in \mathbb{T}$ and $\omega \subseteq \overline{\Omega}$, the patches of order $k \in \mathbb{N}$ inductively by

$$\pi_\bullet^0(\omega) := \omega, \quad \pi_\bullet^k(\omega) := \bigcup \big\{ T \in \mathcal{T}_\bullet : T \cap \pi_\bullet^{k-1}(\omega) \neq \emptyset \big\}. \tag{3.1}$$

The corresponding set of elements is

$$\Pi_\bullet^k(\omega) := \big\{ T \in \mathcal{T}_\bullet : T \subseteq \pi_\bullet^k(\omega) \big\}, \quad \text{i.e.,} \quad \pi_\bullet^k(\omega) = \bigcup \Pi_\bullet^k(\omega) \text{ for } k > 0. \tag{3.2}$$

To abbreviate notation, we let $\pi_\bullet(\omega) := \pi_\bullet^1(\omega)$ and $\Pi_\bullet(\omega) := \Pi_\bullet^1(\omega)$. For $\mathcal{S}_\bullet \subseteq \mathcal{T}_\bullet$, we define $\pi_\bullet^k(\mathcal{S}_\bullet) := \pi_\bullet^k(\bigcup \mathcal{S}_\bullet)$ and $\Pi_\bullet^k(\mathcal{S}_\bullet) := \Pi_\bullet^k(\bigcup \mathcal{S}_\bullet)$.

3.1. Mesh properties

We show that there exist $C_{\text{locuni}}, C_{\text{patch}}, C_{\text{trace}}, C_{\text{dual}} > 0$ such that all meshes $\mathcal{T}_\bullet \in \mathbb{T}$ satisfy the following four properties (**M1**)–(**M4**):

(**M1**) **Local quasi-uniformity.** For all $T \in \mathcal{T}_\bullet$ and all $T' \in \Pi_\bullet(T)$, it holds that $C_{\text{locuni}}^{-1} |T'| \leq |T| \leq C_{\text{locuni}} |T'|$, i.e., neighboring elements have comparable size.

(**M2**) **Bounded element patch.** For all $T \in \mathcal{T}_\bullet$, it holds that $\#\Pi_\bullet(T) \leq C_{\text{patch}}$, i.e., the number of elements in a patch is uniformly bounded.

(**M3**) **Trace inequality.** For all $T \in \mathcal{T}_\bullet$ and all $v \in H^1(\Omega)$, it holds that $\|v\|_{L^2(\partial T)}^2 \leq C_{\text{trace}} \big(|T|^{-1/d} \|v\|_{L^2(T)}^2 + |T|^{1/d} \|\nabla v\|_{L^2(T)}^2 \big)$.

(**M4**) **Local estimate in dual norm:** For all $T \in \mathcal{T}_\bullet$ and all $w \in L^2(T)$, it holds that $|T|^{-1/d} \|w\|_{H^{-1}(T)} \leq C_{\text{dual}} \|w\|_{L^2(T)}$, where $\|w\|_{H^{-1}(T)} := \sup \big\{ \int_T w v \, dx : v \in H_0^1(T) \wedge \|\nabla v\|_{L^2(T)} = 1 \big\}$.

Remark 3.1. In usual applications, where $T \in \mathcal{T}_\bullet$ have simple shapes, the properties (**M3**)–(**M4**) are naturally satisfied; see, e.g., (Gantner, 2017, Section 4.2.1).

To see (**M1**)–(**M4**), let $\mathcal{T}_\bullet \in \mathbb{T}$. Then, (2.24)–(2.25) imply local quasi-uniformity (**M1**) in the parameter domain, which transfers with the help of the regularity (2.31) of γ immediately to the physical domain. The constant C_{locuni} depends only on the dimension d and the constant C_γ. Moreover, (2.24)–(2.25) yield uniform boundedness of the number of elements in a patch, i.e., (**M2**), where C_{patch} depends only on d.

Regularity (2.31) of γ shows that it is sufficient to prove (**M3**) for hyperrectangles $\widehat{T}$ in the parameter domain. There, the trace inequality (**M3**) is well-known; see, e.g., (Gantner, 2017, Proposition 4.2.2) for a proof for general Lipschitz domains. The constant C_{trace} depends only on d and C_γ.

Finally, (**M4**) in the parameter domain follows immediately from the Poincaré inequality. By regularity (2.31) of γ, this property transfers to the physical domain. The constant C_{dual} depends only on d and C_γ.

3.2. Refinement properties

We show that there exist $C_{\text{son}} \geq 2$ and $0 < q_{\text{son}} < 1$ such that all meshes $\mathcal{T}_\bullet \in \mathbb{T}$ satisfy for arbitrary marked elements $\mathcal{M}_\bullet \subseteq \mathcal{T}_\bullet$ with corresponding refinement $\mathcal{T}_\circ := \texttt{refine}(\mathcal{T}_\bullet, \mathcal{M}_\bullet)$, the following elementary properties (**R1**)–(**R3**):

(**R1**) **Bounded number of sons.** It holds that $\#\mathcal{T}_\circ \leq C_{\text{son}} \#\mathcal{T}_\bullet$, i.e., one step of refinement leads to a bounded increase of elements.

(**R2**) **Father is union of sons.** It holds that $T = \bigcup \big\{ T' \in \mathcal{T}_\circ : T' \subseteq T \big\}$ for all $T \in \mathcal{T}_\bullet$, i.e., each element T is the union of its successors.

(**R3**) **Reduction of sons.** It holds that $|T'| \leq q_{\text{son}} |T|$ for all $T \in \mathcal{T}_\bullet$ and all $T' \in \mathcal{T}_\circ$ with $T' \subsetneqq T$, i.e., successors are uniformly smaller than their father.

By induction and the definition of $\texttt{refine}(\mathcal{T}_\bullet)$, one easily sees that (**R2**)–(**R3**) remain valid for arbitrary $\mathcal{T}_\circ \in \texttt{refine}(\mathcal{T}_\bullet)$. In particular, (**R2**)–(**R3**) imply that each refined element $T \in \mathcal{T}_\bullet \setminus \mathcal{T}_\circ$ is split into at least two sons, which is why

$$\#(\mathcal{T}_\bullet \setminus \mathcal{T}_\circ) \leq \#\mathcal{T}_\circ - \#\mathcal{T}_\bullet \quad \text{for all } \mathcal{T}_\circ \in \texttt{refine}(\mathcal{T}_\bullet). \tag{3.3}$$

Remark 3.2. In usual applications, the properties (R2)–(R3) are trivially satisfied. The same holds for (R1) on rectangular meshes. However, (R1) is not obvious for standard refinement strategies for simplicial meshes; see (Gallistl et al., 2014) for 3D newest vertex bisection for tetrahedral meshes.

Moreover, the following properties (R4)–(R5) hold with a generic constant $C_{\mathrm{clos}} > 0$:

(**R4**) **Closure estimate.** If $\mathcal{M}_\ell \subseteq \mathcal{T}_\ell$ and $\mathcal{T}_{\ell+1} = \mathtt{refine}(\mathcal{T}_\ell, \mathcal{M}_\ell)$ for all $\ell \in \mathbb{N}_0$, then

$$\#\mathcal{T}_L - \#\mathcal{T}_0 \leq C_{\mathrm{clos}} \sum_{\ell=0}^{L-1} \#\mathcal{M}_\ell \quad \text{for all } L \in \mathbb{N}.$$

(**R5**) **Overlay estimate.** For all $\mathcal{T}_\bullet, \mathcal{T}_\star \in \mathbb{T}$, there exists a common refinement $\mathcal{T}_\circ \in \mathtt{refine}(\mathcal{T}_\bullet) \cap \mathtt{refine}(\mathcal{T}_\star)$ such that

$$\#\mathcal{T}_\circ \leq \#\mathcal{T}_\bullet + \#\mathcal{T}_\star - \#\mathcal{T}_0.$$

3.2.1. Verification of (R1)–(R3)

(R1) is trivially satisfied with $C_{\mathrm{son}} = 2$, since each refined element is split into exactly two elements. Moreover, the union of sons property (R2) holds by definition. The reduction property (R3) in the parameter domain is trivially satisfied and easily transfers to the physical domain with the help of the regularity (2.31) of γ; see (Gantner et al., 2017, Section 5.3) for details. The constant $0 < q_{\mathrm{son}} < 1$ depends only on d and C_γ.

3.2.2. Verification of (R4)

The proof of the closure estimate (R4) is found in (Morgenstern and Peterseim, 2015, Section 6) for $d = 2$, and in (Morgenstern, 2016, Section 7) for $d = 3$. The constant C_{clos} depends only on the dimension d and the polynomials orders $(p_1, \dots, p_d)$.

3.2.3. Verification of (R5)

The proof of the overlay property (R5) is found in (Morgenstern and Peterseim, 2015, Section 5) for $d = 2$. For $d = 3$, the proof follows along the same lines.

3.3. Space properties

We show that there exist constants $C_{\mathrm{inv}} > 0$ and $k_{\mathrm{loc}}, k_{\mathrm{proj}} \in \mathbb{N}_0$ such that the following properties (S1)–(S3) hold for all $\mathcal{T}_\bullet \in \mathbb{T}$:

(**S1**) **Inverse estimate.** For all $i, j \in \{0, 1, 2\}$ with $j \leq i$, all $V_\bullet \in \mathcal{X}_\bullet$ and all $T \in \mathcal{T}_\bullet$, it holds that $|T|^{(i-j)/d} \|V_\bullet\|_{H^i(T)} \leq C_{\mathrm{inv}} \|V_\bullet\|_{H^j(T)}$.

(**S2**) **Refinement yields nestedness.** For all $\mathcal{T}_\circ \in \mathtt{refine}(\mathcal{T}_\bullet)$, it holds that $\mathcal{X}_\bullet \subseteq \mathcal{X}_\circ$.

(**S3**) **Local domain of definition.** For all $\mathcal{T}_\circ \in \mathtt{refine}(\mathcal{T}_\bullet)$ and all $T \in \mathcal{T}_\bullet \setminus \Pi_\bullet^{k_{\mathrm{loc}}}(\mathcal{T}_\bullet \setminus \mathcal{T}_\circ) \subseteq \mathcal{T}_\bullet \cap \mathcal{T}_\circ$, it holds that $V_\circ|_{\pi_\bullet^{k_{\mathrm{proj}}}(T)} \in \big\{V_\bullet|_{\pi_\bullet^{k_{\mathrm{proj}}}(T)} : V_\bullet \in \mathcal{X}_\bullet\big\}$.

Moreover, we show that there exist $C_{\mathrm{sz}} > 0$ and $k_{\mathrm{app}}, k_{\mathrm{grad}} \in \mathbb{N}_0$ such that for all $\mathcal{T}_\bullet \in \mathbb{T}$, there exists a Scott–Zhang-type projector $J_\bullet : H^1_0(\Omega) \to \mathcal{X}_\bullet$ with the following properties (S4)–(S6):

(**S4**) **Local projection property.** With $k_{\mathrm{proj}} \in \mathbb{N}_0$ from (S3), for all $v \in H^1_0(\Omega)$ and $T \in \mathcal{T}_\bullet$, it holds that $(J_\bullet v)|_T = v|_T$, if $v|_{\pi_\bullet^{k_{\mathrm{proj}}}(T)} \in \big\{V_\bullet|_{\pi_\bullet^{k_{\mathrm{proj}}}(T)} : V_\bullet \in \mathcal{X}_\bullet\big\}$.

(**S5**) **Local L^2-approximation property.** For all $T \in \mathcal{T}_\bullet$ and all $v \in H^1_0(\Omega)$, it holds that $\|(1 - J_\bullet)v\|_{L^2(T)} \leq C_{\mathrm{sz}} |T|^{1/d} \times \|v\|_{H^1(\pi_\bullet^{k_{\mathrm{app}}}(T))}$.

(**S6**) **Local H^1-stability.** For all $T \in \mathcal{T}_\bullet$ and $v \in H^1_0(\Omega)$, it holds that $\|\nabla J_\bullet v\|_{L^2(T)} \leq C_{\mathrm{sz}} \|v\|_{H^1(\pi_\bullet^{k_{\mathrm{grad}}}(T))}$.

3.3.1. Verification of (S1)

Let $T \in \mathcal{T}_\bullet \in \mathbb{T}$. Let $V_\bullet \in \mathcal{X}_\bullet$. Define $\widehat{V}_\bullet := V_\bullet \circ \gamma \in \widehat{\mathcal{X}}_\bullet \subseteq \widehat{\mathcal{Y}}_\bullet$ and $\widehat{T} := \gamma^{-1}(T) \in \widehat{\mathcal{T}}_\bullet$. Regularity (2.31) of γ proves for $i \in \{0, 1, 2\}$ that

$$\|V_\bullet\|_{H^i(T)} \eqsim \|\widehat{V}_\bullet\|_{H^i(\widehat{T})}, \tag{3.4}$$

where the hidden constants depend only on d and C_γ. Thus, it is sufficient to prove (S1) in the parameter domain. In general, $\widehat{V}_\bullet$ is not a $\widehat{\mathcal{T}}_\bullet$-piecewise tensor-polynomial. However, there is a uniform constant $k \in \mathbb{N}_0$ depending only on d and $(p_1, \dots, p_d)$ such that $\widehat{V}_\bullet|_{\widehat{T}'}$ is a tensor-polynomial on any k-times refined son $\widehat{T}' \subseteq \widehat{T}$ with $\widehat{T}' \in \widehat{\mathcal{T}}_{\mathrm{uni}(\mathrm{level}(\widehat{T})+k)}$:

To see this, we use Lemma 2.5, which yields that the number of B-splines $\widehat{B}_{\bullet,z}$ which are needed in the linear combination of $\widehat{V}_\bullet|_{\widehat{T}}$, i.e., $\widehat{B}_{\bullet,z}$ with $|\mathrm{supp}(\widehat{B}_{\bullet,z})\cap\widehat{T}|>0$, is uniformly bounded by k_{supp}. Moreover, Lemma 2.5 and local quasi-uniformity (2.24)–(2.25) show that $\mathrm{level}(\widehat{T}'')\simeq\mathrm{level}(\widehat{T})$ for all elements $\widehat{T}''\in\widehat{\mathcal{T}}_\bullet$ which satisfy that $|\mathrm{supp}(\widehat{B}_{\bullet,z})\cap\widehat{T}''|>0$ for any of these B-splines. Since we only allow dyadic bisections, the definition of $\widehat{B}_{\bullet,z}$ yields the existence of $k\in\mathbb{N}_0$ depending only on d and $(p_1,\dots,p_d)$ such that $\widehat{B}_{\bullet,z}|_{\widehat{T}'}$ and thus $\widehat{V}_\bullet|_{\widehat{T}'}$ are tensor-product polynomials for any son $\widehat{T}'\subseteq\widehat{T}$ with $\widehat{T}'\in\widehat{\mathcal{T}}_{\mathrm{uni}(\mathrm{level}(\widehat{T})+k)}$.

In particular, we can apply a standard scaling argument on $\widehat{T}'$. Since $\widehat{T}$ is the union of all such sons and $|\widehat{T}|\simeq|\widehat{T}'|$, this yields that

$$|\widehat{T}|^{(i-j)/d}\|\widehat{V}_\bullet\|_{H^i(\widehat{T})}\lesssim\|\widehat{V}_\bullet\|_{H^j(\widehat{T})},\tag{3.5}$$

where the hidden constant depends only on d and $(p_1,\dots,p_d)$. Together, (3.4)–(3.5) conclude the proof of (**S1**), where C_{inv} depends only on d, C_γ, and $(p_1,\dots,p_d)$.

3.3.2. Verification of (S2)

We note that in general, i.e., for arbitrary T-meshes, nestedness of the induced T-splines spaces is not evident; see, e.g., (Li and Scott, 2014, Section 6). However, the refinement strategies (Algorithm 2.1) from (Morgenstern and Peterseim, 2015; Morgenstern, 2016) yield nested T-spline spaces. For $d=2$, this is stated in (Morgenstern and Peterseim, 2015, Corollary 5.8). For $d=3$, this is stated in (Morgenstern, 2017, Theorem 5.4.12). We already mentioned in Section 2.3 that (Morgenstern, 2016) (as well as (Morgenstern, 2017)) define the space of T-splines differently as the span of $\{\widehat{B}_{\bullet,z}:z\in\widehat{\mathcal{N}}_\bullet^{\mathrm{act}}\cap\widetilde{\widehat{\Omega}}\}$. Nevertheless, the proofs immediately generalize to our standard definition of T-splines, i.e.,

$$\widehat{\mathcal{Y}}_\bullet\subseteq\widehat{\mathcal{Y}}_\circ\quad\text{for all }\widehat{\mathcal{T}}_\bullet\in\mathbb{T},\widehat{\mathcal{T}}_\circ\in\mathtt{refine}(\widehat{\mathcal{T}}_\bullet),\tag{3.6}$$

which also yields the inclusion $\mathcal{X}_\bullet\subseteq\mathcal{X}_\circ$.

3.3.3. Verification of (S3)

We show the assertion in the parameter domain. For arbitrary but fixed $k_{\mathrm{proj}}\in\mathbb{N}_0$ (which will be fixed later in Section 3.3.4 to be $k_{\mathrm{proj}}:=k_{\mathrm{supp}}$), we set $k_{\mathrm{loc}}:=k_{\mathrm{proj}}+k_{\mathrm{supp}}$ with k_{supp} from Lemma 2.5. Let $\widehat{\mathcal{T}}_\bullet\in\widehat{\mathbb{T}}$, $\widehat{\mathcal{T}}_\circ\in\mathtt{refine}(\widehat{\mathcal{T}}_\bullet)$, and $\widehat{V}_\circ\in\widehat{\mathcal{X}}_\circ$. We define the patch functions $\pi_\bullet(\cdot)$ and $\Pi_\bullet(\cdot)$ in the parameter domain analogously to the patch functions in the physical domain. Let $\widehat{T}\in\widehat{\mathcal{T}}_\bullet\setminus\Pi_\bullet^{k_{\mathrm{loc}}}(\widehat{\mathcal{T}}_\bullet\setminus\widehat{\mathcal{T}}_\circ)$. Then, one easily shows that

$$\Pi_\bullet^{k_{\mathrm{loc}}}(\widehat{T})\subseteq\widehat{\mathcal{T}}_\bullet\cap\widehat{\mathcal{T}}_\circ;\tag{3.7}$$

see (Gantner et al., 2017, Section 5.8). We see that $\widehat{\omega}=\pi_\circ^{k_{\mathrm{loc}}}(\widehat{T})$, and, in particular, also $\widehat{\omega}:=\pi_\bullet^{k_{\mathrm{proj}}}(\widehat{T})=\pi_\circ^{k_{\mathrm{proj}}}(\widehat{T})$. According to Lemma 2.4, it holds that

$$\{\widehat{V}_\bullet|_{\widehat{\omega}}:\widehat{V}_\bullet\in\widehat{\mathcal{X}}_\bullet\}=\mathrm{span}\{\widehat{B}_{\bullet,z}|_{\widehat{\omega}}:\big(z\in\widehat{\mathcal{N}}_\bullet^{\mathrm{act}}\setminus\partial\widehat{\Omega}^{\mathrm{act}}\big)\wedge\big(|\mathrm{supp}(\widehat{B}_{\bullet,z})\cap\widehat{\omega}|>0\big)\},$$

as well as

$$\{\widehat{V}_\circ|_{\widehat{\omega}}:\widehat{V}_\circ\in\widehat{\mathcal{X}}_\circ\}=\mathrm{span}\{\widehat{B}_{\circ,z}|_{\widehat{\omega}}:\big(z\in\widehat{\mathcal{N}}_\circ^{\mathrm{act}}\setminus\partial\widehat{\Omega}^{\mathrm{act}}\big)\wedge\big(|\mathrm{supp}(\widehat{B}_{\circ,z})\cap\widehat{\omega}|>0\big)\}.$$

We will prove that

$$\{\widehat{B}_{\bullet,z}:z\in\widehat{\mathcal{N}}_\bullet^{\mathrm{act}}\wedge|\mathrm{supp}(\widehat{B}_{\bullet,z})\cap\widehat{\omega}|>0\}=\{\widehat{B}_{\circ,z}:z\in\widehat{\mathcal{N}}_\circ^{\mathrm{act}}\wedge|\mathrm{supp}(\widehat{B}_{\circ,z})\cap\widehat{\omega}|>0\},\tag{3.8}$$

which will conclude (**S3**). To show "$\subseteq$", let $\widehat{B}_{\bullet,z}$ be an element of the left set. By Lemma 2.5, this implies that $\mathrm{supp}(\widehat{B}_{\bullet,z})\subseteq\pi_\bullet^{k_{\mathrm{loc}}}(\widehat{T})$. Together with (3.7), we see that $\mathrm{supp}(\widehat{B}_{\bullet,z})\subseteq\bigcup(\widehat{\mathcal{T}}_\bullet\cap\widehat{\mathcal{T}}_\circ)$. This proves that no element within $\mathrm{supp}(\widehat{B}_{\bullet,z})$ is changed during refinement. Thus, the definition of T-spline basis functions proves that $\widehat{B}_{\bullet,z}=\widehat{B}_{\circ,z}$. The same argument shows the converse inclusion "$\supseteq$". This proves (3.8), and thus (**S3**) follows.

3.3.4. Verification of (S4)–(S6)

Given $\mathcal{T}_\bullet\in\mathbb{T}$, we introduce a suitable Scott–Zhang-type operator $J_\bullet:H^1_0(\Omega)\to\mathcal{X}_\bullet$ which satisfies (**S4**)–(**S6**). To this end, it is sufficient to construct a corresponding operator $\widehat{J}_\bullet:H^1_0(\widehat{\Omega})\to\widehat{\mathcal{X}}_\bullet$ in the parameter domain, and to define

$$J_\bullet v:=\big(\widehat{J}_\bullet(v\circ\gamma)\big)\circ\gamma^{-1}\quad\text{for all }v\in H^1_0(\Omega).\tag{3.9}$$

By regularity (2.31) of γ, the properties (**S4**)–(**S6**) immediately transfer from the parameter domain $\widehat{\Omega}$ to the physical domain Ω. In Section 2.3, we have already mentioned that any admissible mesh $\widehat{\mathcal{T}}_\bullet\in\widehat{\mathbb{T}}$ yields dual-compatible B-splines $\{\widehat{B}_{\bullet,z}:z\in\widehat{\mathcal{N}}_\bullet^{\mathrm{act}}\}$. According to (Beirão da Veiga et al., 2014, Section 2.1.5) in combination with (Beirão da Veiga et al., 2014, Proposition 7.3) for $d=2$ and with (Morgenstern, 2016, Theorem 6.7) for $d=3$, this implies for all $z\in\widehat{\mathcal{N}}_\bullet$ the existence of a local dual function $\widehat{B}^*_{\bullet,z}\in L^2(\widehat{\Omega})$ with $\mathrm{supp}(\widehat{B}^*_{\bullet,z})=\mathrm{supp}(\widehat{B}_{\bullet,z})$ such that

$$\int_{\widehat{\Omega}} \widehat{B}^*_{\bullet,z}\,\widehat{B}_{\bullet,z'}\,dt = \delta_{z,z'} \quad \text{for all } z' \in \widehat{\mathcal{N}}^{\mathrm{act}}_\bullet, \tag{3.10}$$

and

$$\|\widehat{B}^*_{\bullet,z}\|_{L^2(\widehat{\Omega})} \le \prod_{i=1}^{d} \big(9^{p_i}(2p_i+3)^d\big)\,|\mathrm{supp}(\widehat{B}_{\bullet,z})|^{-1/2}. \tag{3.11}$$

With these dual functions, it is easy to define a suitable Scott–Zhang-type operator by

$$\widehat{J}_\bullet : L^2(\widehat{\Omega}) \to \widehat{\mathcal{X}}_\bullet, \quad \widehat{v} \mapsto \sum_{z \in \widehat{\mathcal{N}}^{\mathrm{act}}_\bullet \setminus \partial\widehat{\Omega}^{\mathrm{act}}} \Big(\int_{\widehat{\Omega}} \widehat{B}^*_{\bullet,z}\,\widehat{v}\,dt \Big)\,\widehat{B}_{\bullet,z}. \tag{3.12}$$

A similar operator has already been defined and analyzed, e.g., in (Beirão da Veiga et al., 2014, Section 7.1). Indeed, the only difference in the definition is the considered index set $\widehat{\mathcal{N}}^{\mathrm{act}}_\bullet \setminus \partial\widehat{\Omega}^{\mathrm{act}}$ instead of $\widehat{\mathcal{N}}^{\mathrm{act}}_\bullet$, which guarantees that $\widehat{J}_\bullet\widehat{v}$ vanishes on the boundary; see Lemma 2.4. Along the lines of (Beirão da Veiga et al., 2014, Proposition 7.7), one can thus prove the following result, where the projection property (3.13) follows immediately from (3.10).

Lemma 3.3. *Let $\widehat{\mathcal{T}}_\bullet \in \widehat{\mathbb{T}}$. Then, $\widehat{J}_\bullet$ is a projection, i.e.,*

$$\widehat{J}_\bullet \widehat{V}_\bullet = \widehat{V}_\bullet \quad \textit{for all } \widehat{V}_\bullet \in \mathcal{X}_\bullet. \tag{3.13}$$

Moreover, $\widehat{J}_\bullet$ is locally L^2-stable, i.e., there exists $C_J > 0$ such that for all $\widehat{T} \in \widehat{\mathcal{T}}_\bullet$

$$\|\widehat{J}_\bullet\widehat{v}\|_{L^2(\widehat{T})} \le C_J \|\widehat{v}\|_{L^2(\bigcup\{\mathrm{supp}(\widehat{B}_{\bullet,z}) : (z \in \mathcal{N}^{\mathrm{act}}_\bullet \setminus \partial\widehat{\Omega}^{\mathrm{act}}) \wedge |\mathrm{supp}(\widehat{B}_{\bullet,z}) \cap \widehat{T}| > 0\})} \quad \textit{for all } \widehat{v} \in L^2(\widehat{\Omega}). \tag{3.14}$$

The constant C_J depends only on d and $(p_1, \dots, p_d)$. □

With Lemma 3.3 at hand, we next prove (**S4**) in the parameter domain. Let $\widehat{T} \in \widehat{\mathcal{T}}_\bullet$, $\widehat{v} \in H^1_0(\widehat{\Omega})$, and $\widehat{V}_\bullet \in \widehat{\mathcal{X}}_\bullet$ such that $\widehat{v}|_{\pi_\bullet^{k_{\mathrm{proj}}}(\widehat{T})} = \widehat{V}_\bullet|_{\pi_\bullet^{k_{\mathrm{proj}}}(\widehat{T})}$, where $k_{\mathrm{proj}} := k_{\mathrm{supp}}$ with k_{supp} from Lemma 2.5. With Lemma 2.5, the fact that $\mathrm{supp}(\widehat{B}^*_{\bullet,z}) = \mathrm{supp}(\widehat{B}_{\bullet,z})$, and the projection property (3.13) of $\widehat{J}_\bullet$, we conclude that

$$(\widehat{J}_\bullet\widehat{v})|_{\widehat{T}} = \sum_{z \in \widehat{\mathcal{N}}^{\mathrm{act}}_\bullet \setminus \partial\widehat{\Omega}^{\mathrm{act}}} \Big(\int_{\widehat{\Omega}} \widehat{B}^*_{\bullet,z}\,\widehat{v}\,dt \Big)\,\widehat{B}_{\bullet,z}|_{\widehat{T}} = \sum_{\substack{z \in \widehat{\mathcal{N}}^{\mathrm{act}}_\bullet \setminus \partial\widehat{\Omega}^{\mathrm{act}} \\ \mathrm{supp}(\widehat{B}_{\bullet,z}) \subseteq \pi_\bullet^{\mathrm{proj}}(\widehat{T})}} \Big(\int_{\widehat{\Omega}} \widehat{B}^*_{\bullet,z}\,\widehat{V}_\bullet\,dt \Big)\,\widehat{B}_{\bullet,z}|_{\widehat{T}} = \widehat{V}_\bullet|_{\widehat{T}} = \widehat{v}|_{\widehat{T}}.$$

Next, we prove (**S5**). We note that for the modified projection operator from (Beirão da Veiga et al., 2014), this property is already found, e.g., in (Beirão da Veiga et al., 2014, Proposition 7.8). Let $\widehat{T} \in \widehat{\mathcal{T}}_\bullet$, $\widehat{v} \in H^1_0(\widehat{\Omega})$, and $\widehat{V}_\bullet \in \widehat{\mathcal{X}}_\bullet$. By (3.13)–(3.14) and Lemma 2.5, it holds that

$$\|(1-\widehat{J}_\bullet)\widehat{v}\|_{L^2(\widehat{T})} \overset{(3.13)}{=} \|(1-\widehat{J}_\bullet)(\widehat{v}-\widehat{V}_\bullet)\|_{L^2(\widehat{T})} \overset{(3.14)}{\lesssim} \|\widehat{v}-\widehat{V}_\bullet\|_{L^2(\pi_\bullet^{k_{\mathrm{supp}}}(\widehat{T}))}.$$

To proceed, we distinguish between two cases, first, $\pi_\bullet^{2k_{\mathrm{supp}}}(\widehat{T}) \cap \partial\widehat{\Omega} = \emptyset$ and, second, $\pi_\bullet^{2k_{\mathrm{supp}}}(\widehat{T}) \cap \partial\widehat{\Omega} \neq \emptyset$, i.e., if $\widehat{T}$ is far away from the boundary or not. Since the elements in the parameter domain are hyperrectangular, these cases are equivalent to $|\pi_\bullet^{2k_{\mathrm{supp}}}(\widehat{T}) \cap \partial\widehat{\Omega}| = 0$ and $|\pi_\bullet^{2k_{\mathrm{supp}}}(\widehat{T}) \cap \partial\widehat{\Omega}| > 0$, respectively, where $|\cdot|$ denotes the $(d-1)$-dimensional measure.

In the first case, we proceed as follows: Nestedness (3.6) especially proves that $1 \in \widehat{\mathcal{Y}}_0 \subseteq \widehat{\mathcal{Y}}_\bullet$. Thus, there exists a representation $1 = \sum_{z \in \widehat{\mathcal{N}}^{\mathrm{act}}_\bullet} c_z \widehat{B}_{\bullet,z}$. Indeed, (Beirão da Veiga et al., 2014, Proposition) even proves that $c_z = 1$ for all $z \in \widehat{\mathcal{N}}^{\mathrm{act}}_\bullet$, i.e., the B-splines $\{\widehat{B}_{\bullet,z} : z \in \widehat{\mathcal{N}}^{\mathrm{act}}_\bullet\}$ form a partition of unity. With Lemma 2.5, we see that $|\mathrm{supp}(\widehat{\beta}) \cap \pi_\bullet^{k_{\mathrm{supp}}}(\widehat{T})| > 0$ implies that $\mathrm{supp}(\widehat{\beta}) \subseteq \pi_\bullet^{2k_{\mathrm{supp}}}(\widehat{T})$. Therefore, the restriction satisfies that

$$1 = \sum_{z \in \widehat{\mathcal{N}}^{\mathrm{act}}_\bullet} \widehat{B}_{\bullet,z}|_{\pi_\bullet^{k_{\mathrm{supp}}}(\widehat{T})} = \sum_{\substack{z \in \widehat{\mathcal{N}}^{\mathrm{act}}_\bullet \\ |\mathrm{supp}(\widehat{B}_{\bullet,z}) \cap \pi_\bullet^{k_{\mathrm{supp}}}(\widehat{T})| > 0}} \widehat{B}_{\bullet,z}|_{\pi_\bullet^{k_{\mathrm{supp}}}(\widehat{T})} = \sum_{\substack{z \in \widehat{\mathcal{N}}^{\mathrm{act}}_\bullet \\ \mathrm{supp}(\widehat{B}_{\bullet,z}) \subseteq \pi_\bullet^{2k_{\mathrm{supp}}}(\widehat{T})}} \widehat{B}_{\bullet,z}|_{\pi_\bullet^{k_{\mathrm{supp}}}(\widehat{T})}.$$

We define

$$\widehat{V}_\bullet := \widehat{v}_{\pi_\bullet^{k_{\mathrm{supp}}}(\widehat{T})} \sum_{\substack{z \in \widehat{\mathcal{N}}^{\mathrm{act}}_\bullet \\ \mathrm{supp}(\widehat{B}_{\bullet,z}) \subseteq \pi_\bullet^{2k_{\mathrm{supp}}}(\widehat{T})}} \widehat{B}_{\bullet,z}, \quad \text{where } \widehat{v}_{\pi_\bullet^{k_{\mathrm{supp}}}(\widehat{T})} := |\pi_\bullet^{k_{\mathrm{supp}}}(\widehat{T})|^{-1} \int_{\pi_\bullet^{k_{\mathrm{supp}}}(\widehat{T})} \widehat{v}\,dt.$$

In the second case, we set $\widehat{V}_\bullet := 0$. In the first case, we apply the Poincaré inequality, whereas we use the Friedrichs inequality in the second case. In either case, we obtain that $\widehat{V}_\bullet \in \widehat{\mathcal{X}}_\bullet$, and (2.24)–(2.25) show that

$$\|\widehat{v} - \widehat{V}_\bullet\|_{L^2(\pi_\bullet^{k_{\mathrm{supp}}}(\widehat{T}))} \lesssim \operatorname{diam}(\pi_\bullet^{2k_{\mathrm{supp}}}(\widehat{T}))\|\nabla\widehat{v}\|_{L^2(\pi_\bullet^{2k_{\mathrm{supp}}}(\widehat{T}))} \simeq |\widehat{T}|^{1/d}\|\nabla\widehat{v}\|_{L^2(\pi_\bullet^{2k_{\mathrm{supp}}}(\widehat{T}))}. \tag{3.15}$$

The hidden constants depend only on $\widehat{\mathcal{T}}_0$, $(p_1, \dots, p_d)$, and the shape of the patch $\pi_\bullet^{k_{\mathrm{supp}}}(\widehat{T})$ or the shape of $\pi_\bullet^{2k_{\mathrm{supp}}}(\widehat{T})$ and of $\pi_\bullet^{k_{\mathrm{supp}}}(\widehat{T}) \cap \partial\widehat{\Omega}$. However, by (2.24)–(2.25), the number of different patch shapes is bounded itself by a constant which again depends only on d and $(p_1, \dots, p_d)$.

Finally, we prove (**S6**). Let again $\widehat{T} \in \widehat{\mathcal{T}}_\bullet$ and $\widehat{v} \in H^1_0(\widehat{\Omega})$. For all $\widehat{V}_\bullet \in \widehat{\mathcal{X}}_\bullet$ that are constant on $\widehat{T}$, the projection property (3.13) implies that

$$\begin{aligned}\|\nabla\widehat{J}_\bullet\widehat{v}\|_{L^2(\widehat{T})} &\overset{(3.13)}{=} \|\nabla\widehat{J}_\bullet(\widehat{v} - \widehat{V}_\bullet)\|_{L^2(\widehat{T})} \overset{(3.5)}{\lesssim} |\widehat{T}|^{-1/d}\,\|\widehat{J}_\bullet(v - \widehat{V}_\bullet)\|_{L^2(\widehat{T})} \\ &\overset{(3.14)}{\lesssim} |\widehat{T}|^{-1/d}\,\|\widehat{v} - \widehat{V}_\bullet\|_{L^2(\pi_\bullet^{k_{\mathrm{supp}}}(\widehat{T}))}.\end{aligned}$$

Arguing as before and using (3.15), we conclude the proof.

3.4. Oscillation properties

There exists $C'_{\mathrm{inv}} > 0$ such that the following property (**O1**) holds for all $\mathcal{T}_\bullet \in \mathbb{T}$:

(**O1**) **Inverse estimate in dual norm.** For all $W \in \mathcal{P}(\Omega)$, it holds that $|T|^{1/d}\|W\|_{L^2(T)} \le C'_{\mathrm{inv}}\|W\|_{H^{-1}(T)}$.

Moreover, there exists $C_{\mathrm{lift}} > 0$ such that for all $\mathcal{T}_\bullet \in \mathbb{T}$ and all $T, T' \in \mathcal{T}_\bullet$ with non-trivial $(d-1)$-dimensional intersection $E := T \cap T'$, there exists a lifting operator $L_{\bullet,E} : \{W|_E : W \in \mathcal{P}(\Omega)\} \to H^1_0(T \cup T')$ with the following properties (**O2**)–(**O4**):

(**O2**) **Lifting inequality.** For all $W \in \mathcal{P}(\Omega)$, it holds that $\int_E W^2\,dx \le C_{\mathrm{lift}}\int_E L_{\bullet,E}(W|_E)W\,dx$.
(**O3**) $\boldsymbol{L^2}$**-control.** For all $W \in \mathcal{P}(\Omega)$, it holds that $\|L_{\bullet,E}(W|_E)\|^2_{L^2(T\cup T')} \le C_{\mathrm{lift}}|T \cup T'|^{1/d}\|W\|^2_{L^2(E)}$.
(**O4**) $\boldsymbol{H^1}$**-control.** For all $W \in \mathcal{P}(\Omega)$, it holds that $\|\nabla L_{\bullet,E}(W|_E)\|^2_{L^2(T\cup T')} \le C_{\mathrm{lift}}|T \cup T'|^{-1/d}\|W\|^2_{L^2(E)}$.

The properties can be proved along the lines of (Gantner et al., 2017, Section 5.11–5.12), where they are proved for polynomials on hierarchical meshes; see also (Gantner, 2017, Section 4.5.11–4.5.12) for details. The proofs rely on standard scaling arguments and the existence of a suitable bubble function. The involved constants thus depend only on d, C_γ, and $(q_1, \dots, q_d)$.

4. Possible generalizations

In this section, we briefly discuss several easy generalizations of Theorem 2.11. We note that all following generalizations are compatible with each other, i.e., Theorem 2.11 holds analogously for rational T-splines in arbitrary dimension $d \ge 2$ on geometries Ω that are initially non-uniformly meshed if one uses arbitrarily graded mesh-refinement. If $d = 2$, one can even employ rational T-splines of arbitrary degree $p_1, p_2 \ge 2$.

4.1. Rational T-splines

Instead of the ansatz space $\mathcal{X}_\bullet$, one can use rational hierarchical splines, i.e.,

$$\mathcal{X}_\bullet^{W_0} := \left\{\frac{V_\bullet}{W_0} : V_\bullet \in \mathcal{X}_\bullet\right\}, \tag{4.1}$$

where $W_0 \in \mathcal{Y}_0$ with $W_0 > 0$ is a fixed positive weight function. In this case, the corresponding basis consists of NURBS instead of B-splines. Indeed, the mesh properties (**M1**)–(**M4**), the refinement properties (**R1**)–(**R5**), and the oscillation properties (**O1**)–(**O4**) from Section 3 are independent of the discrete spaces. To verify the validity of Theorem 2.11 in the NURBS setting, it thus only remains to verify the properties (**S1**)–(**S6**) for the NURBS finite element spaces. The inverse estimate (**S1**) follows similarly as in Section 3.3 since we only consider a fixed and thus uniformly bounded weight function $W_0 \in \mathcal{Y}_0$. The properties (**S2**)–(**S3**) depend only on the numerator of the NURBS functions and thus transfer. To see (**S4**)–(**S6**), one can proceed as in Section 3.3, where the corresponding Scott–Zhang-type operator $J_\bullet^{W_0} : L^2(\Omega) \to \mathcal{X}_\bullet^{W_0}$ now reads $J_\bullet^{W_0}v := J_\bullet(vW_0)/W_0$ for all $v \in L^2(\Omega)$. Overall, the involved constants then depend additionally on W_0.

4.2. Non-uniform initial mesh

By definition, $\widehat{\mathcal{T}}_0$ is a uniform tensor-mesh. Instead one can also allow for non-uniform tensor-meshes

$$\widehat{\mathcal{T}}_0 = \Big\{ \prod_{i=1}^{d} [a_{i,j}, a_{i,j+1}] : i \in \{1,\dots,d\} \wedge j \in \{0,\dots,N_i-1\} \Big\}, \tag{4.2}$$

where $(a_{i,j})_{j=0}^{N_i}$ is a strictly increasing vector with $a_{i,0} = 0$ and $a_{i,N_i} = N_i$, and adapt the corresponding definitions accordingly. In particular, for the refinement, the definition (2.18) of neighbors of an element has to be adapted and depends on $\widehat{\mathcal{T}}_0$. To circumvent this problem, one can transform the non-uniform mesh via some function φ to a uniform one, perform the refinement there, and then transform the refined mesh back via φ^{-1}. Indeed, for each $i \in \{1,\dots,d\}$, there exists a continuous strictly monotonously increasing function $\varphi_i : [0, N_i] \to [0, N_i]$ that affinely maps any interval $[a_{i,j}, a_{i,j+1}]$ to $[j, j+1]$. Then, the resulting tensor-product $\varphi := \varphi_1 \otimes \cdots \otimes \varphi_d : \overline{\widehat{\Omega}} \to \overline{\widehat{\Omega}}$ defined as in (2.15) is a bijection. To prove the mesh properties (**M1**)–(**M4**) and the refinement properties (**R1**)–(**R5**), one first verifies them on transformed meshes $\{\varphi(\widehat{T}) : \widehat{T} \in \widehat{\mathcal{T}}_\bullet\}$ as in Section 3.1–3.2, and then transforms these results via $\gamma \circ \varphi^{-1}$ to physical meshes $\mathcal{T}_\bullet$. The space properties (**S1**)–(**S6**) and the oscillation properties (**O1**)–(**O4**) follow as in Section 3.3–3.4. All involved constants depend additionally on $\widehat{\mathcal{T}}_0$.

4.3. Arbitrary grading

Instead of dividing the refined elements into two sons, one can also divide them into m sons, where $m \geq 2$ is a fixed integer. Indeed, such a grading parameter n has already been proposed and analyzed in (Morgenstern, 2016) to obtain a more localized refinement strategy. The proofs hold verbatim, but the constants depend additionally on m.

4.4. Arbitrary dimension $d \geq 2$

(Morgenstern, 2017, Section 5.4 and 5.5) generalizes T-meshes, T-splines, and the refinement strategy developed in (Morgenstern, 2016) for $d = 3$ to arbitrary $d \geq 2$. We note that the resulting refinement for $d = 2$ does not coincide with the refinement from (Morgenstern and Peterseim, 2015) that we consider in this work. Instead, the latter leads to a smaller mesh closure. However, Theorem 2.11 is still valid if the refinement strategy from (Morgenstern, 2017, Section 5.4 and 5.5) is used for $d \geq 2$. Indeed, the mesh properties (**M1**)–(**M4**) essentially follow from (2.24)–(2.25), which are stated in (Morgenstern, 2017, Lemma 5.4.10). The properties (**R1**)–(**R3**) are satisfied by definition, (**R4**) is proved in (Morgenstern, 2017, Section 5.4.2), and (**R5**) follows along the lines of (Morgenstern and Peterseim, 2015, Section 5). The space properties (**S1**) and (**S3**)–(**S6**) can be verified as in Section 3.3, where the required dual-compatibility is found in (Morgenstern, 2017, Theorem 5.3.14 and 5.4.11). Nestedness (**S2**) is proved in (Morgenstern, 2017, Theorem 5.4.12). The oscillation properties (**O1**)–(**O4**) follow as in Section 3.4.

4.5. Arbitrary polynomial degrees $(p_1,\dots,p_d)$ for $d = 2$

In (Beirão da Veiga et al., 2013), T-splines of arbitrary degree have been analyzed for $d = 2$. Depending on the degrees $p_1, p_2 \geq 2$, the corresponding basis functions are associated with elements, element edges, or, as in our case, with nodes. We only restricted to odd degrees for the sake of readability. Indeed, the work (Morgenstern and Peterseim, 2015) allows for arbitrary $p_1, p_2 \geq 2$. In particular, all cited results of (Morgenstern and Peterseim, 2015) are also valid in this case, and Theorem 2.11 follows along the lines of Section 3. However, to the best of our knowledge, T-splines of arbitrary degree have not been investigated for $d > 2$.

Declaration of competing interest

The authors declare that they have no known competing financial interests or personal relationships that could have appeared to influence the work reported in this paper.

Acknowledgement

The authors acknowledge support through the Austrian Science Fund (FWF) under grants P29096, W1245 and J4379.

References

Ainsworth, Mark, Oden, J. Tinsley, 2000. A Posteriori Error Estimation in Finite Element Analysis. Pure and Applied Mathematics (New York). John Wiley & Sons, New York.

Bazilevs, Yuri, Beirão da Veiga, Lourenco, Cottrell, J. Austin, Hughes, Thomas J.R., Sangalli, Giancarlo, 2006. Isogeometric analysis: approximation, stability and error estimates for h-refined meshes. Math. Models Methods Appl. Sci. 16 (07), 1031–1090.

Beirão da Veiga, Lourenco, Buffa, Annalisa, Sangalli, Giancarlo, Vázquez, Rafael, 2013. Analysis-suitable T-splines of arbitrary degree: definition, linear independence and approximation properties. Math. Models Methods Appl. Sci. 23 (11), 1979–2003.
Beirão da Veiga, Lourenco, Buffa, Annalisa, Sangalli, Giancarlo, Vázquez, Rafael, 2014. Mathematical analysis of variational isogeometric methods. Acta Numer. 23, 157–287.
Bespalov, Alex, Haberl, Alexander, Praetorius, Dirk, 2017. Adaptive FEM with coarse initial mesh guarantees optimal convergence rates for compactly perturbed elliptic problems. Comput. Methods Appl. Mech. Eng. 317, 318–340.
Binev, Peter, Dahmen, Wolfgang, DeVore, Ron, 2004. Adaptive finite element methods with convergence rates. Numer. Math. 97 (2), 219–268.
Bracco, Cesare, Buffa, Annalisa, Giannelli, Carlotta, Vázquez, Rafael, 2019. Adaptive isogeometric methods with hierarchical splines: an overview. Discrete Contin. Dyn. Syst. 39 (1), 241–261.
Buffa, Annalisa, Garau, Eduardo M., 2018. A posteriori error estimators for hierarchical B-spline discretizations. Math. Models Methods Appl. Sci. 28 (8), 1453–1480.
Buffa, Annalisa, Giannelli, Carlotta, 2016. Adaptive isogeometric methods with hierarchical splines: error estimator and convergence. Math. Models Methods Appl. Sci. 26 (01), 1–25.
Buffa, Annalisa, Giannelli, Carlotta, 2017. Adaptive isogeometric methods with hierarchical splines: optimality and convergence rates. Math. Models Methods Appl. Sci. 27 (14), 2781–2802.
Buffa, Annalisa, Cho, Durkbin, Sangalli, Giancarlo, 2010. Linear independence of the T-spline blending functions associated with some particular T-meshes. Comput. Methods Appl. Mech. Eng. 199 (23–24), 1437–1445.
Carstensen, Carsten, Feischl, Michael, Page, Marcus, Praetorius, Dirk, 2014. Axioms of adaptivity. Comput. Math. Appl. 67 (6), 1195–1253.
Cascon, J. Manuel, Kreuzer, Christian, Nochetto, Ricardo H., Siebert, Kunibert G., 2008. Quasi-optimal convergence rate for an adaptive finite element method. SIAM J. Numer. Anal. 46 (5), 2524–2550.
Cho, Durkbin, Vázquez, Rafael, 2020. BPX preconditioners for isogeometric analysis using analysis-suitable T-splines. IMA J. Numer. Anal. 40 (1), 764–799.
Cottrell, J. Austin, Hughes, Thomas J.R., Bazilevs, Yuri, 2009. Isogeometric Analysis: Toward Integration of CAD and FEA. John Wiley & Sons, New York.
de Boor, Carl, 2001. A Practical Guide to Splines. Springer, New York.
Dokken, Tor, Lyche, Tom, Pettersen, Kjell F., 2013. Polynomial splines over locally refined box-partitions. Comput. Aided Geom. Des. 30 (3), 331–356.
Dörfel, Michael R., Jüttler, Bert, Simeon, Bernd, 2010. Adaptive isogeometric analysis by local h-refinement with T-splines. Comput. Methods Appl. Mech. Eng. 199 (5–8), 264–275.
Dörfler, Willy, 1996. A convergent adaptive algorithm for Poisson's equation. SIAM J. Numer. Anal. 33 (3), 1106–1124.
Feischl, Michael, Führer, Thomas, Praetorius, Dirk, 2014. Adaptive FEM with optimal convergence rates for a certain class of nonsymmetric and possibly nonlinear problems. SIAM J. Numer. Anal. 52 (2), 601–625.
Feischl, Michael, Gantner, Gregor, Praetorius, Dirk, 2015. Reliable and efficient a posteriori error estimation for adaptive IGA boundary element methods for weakly-singular integral equations. Comput. Methods Appl. Mech. Eng. 290, 362–386.
Feischl, Michael, Gantner, Gregor, Haberl, Alexander, Praetorius, Dirk, 2016. Adaptive 2D IGA boundary element methods. Eng. Anal. Bound. Elem. 62, 141–153.
Feischl, Michael, Gantner, Gregor, Haberl, Alexander, Praetorius, Dirk, 2017. Optimal convergence for adaptive IGA boundary element methods for weakly-singular integral equations. Numer. Math. 136 (1), 147–182.
Führer, Thomas, Haberl, Alexander, Praetorius, Dirk, Schimanko, Stefan, 2019. Adaptive BEM with inexact PCG solver yields almost optimal computational costs. Numer. Math. 141, 967–1008.
Gallistl, Dietmar, Schedensack, Mira, Stevenson, Rob P., 2014. A remark on newest vertex bisection in any space dimension. Comput. Methods Appl. Math. 14 (3), 317–320.
Gantner, Gregor, 2017. Optimal adaptivity for splines in finite and boundary element methods. PhD thesis. Institute for Analysis and Scientific Computing, TU Wien.
Gantner, Gregor, Haberlik, Daniel, Praetorius, Dirk, 2017. Adaptive IGAFEM with optimal convergence rates: hierarchical B-splines. Math. Models Methods Appl. Sci. 27 (14), 2631–2674.
Gantner, Gregor, Praetorius, Dirk, Schimanko, Stefan, 2020a. Adaptive isogeometric boundary element methods with local smoothness control. Math. Models Methods Appl. Sci. 30 (2), 261–307.
Gantner, Gregor, Haberl, Alexander, Praetorius, Dirk, Schimanko, Stefan, 2020b. Rate optimality of adaptive finite element methods with respect to the overall computational costs. arXiv preprint. arXiv:2003.10785.
Gaspoz, Fernando D., Morin, Pedro, 2008. Convergence rates for adaptive finite elements. IMA J. Numer. Anal. 29 (4), 917–936.
Giannelli, Carlotta, Jüttler, Bert, Speleers, Hendrik, 2012. THB-splines: the truncated basis for hierarchical splines. Comput. Aided Geom. Des. 29 (7), 485–498.
Golub, Gene H., van Loan, Charles F., 2012. Matrix Computations, Vol. 4. Johns Hopkins University Press, Baltimore.
Hennig, Paul, Kästner, Markus, Morgenstern, Philipp, Peterseim, Daniel, 2017. Adaptive mesh refinement strategies in isogeometric analysis—a computational comparison. Comput. Methods Appl. Mech. Eng. 316, 424–448.
Hughes, Thomas J.R., Cottrell, J. Austin, Bazilevs, Yuri, 2005. Isogeometric analysis: CAD, finite elements, NURBS, exact geometry and mesh refinement. Comput. Methods Appl. Mech. Eng. 194 (39), 4135–4195.
Johannessen, Kjetil A., Kvamsdal, Trond, Dokken, Tor, 2014. Isogeometric analysis using LR B-splines. Comput. Methods Appl. Mech. Eng. 269, 471–514.
Johannessen, Kjetil A., Remonato, Filippo, Kvamsdal, Trond, 2015. On the similarities and differences between classical hierarchical, truncated hierarchical and LR B-splines. Comput. Methods Appl. Mech. Eng. 291, 64–101.
Kuru, Gokturk, Verhoosel, Clemens V., Van der Zee, Kristoffer G., van Brummelen, E. Harald, 2014. Goal-adaptive isogeometric analysis with hierarchical splines. Comput. Methods Appl. Mech. Eng. 270, 270–292.
Li, Xin, Scott, Michael A., 2014. Analysis-suitable T-splines: characterization, refineability, and approximation. Math. Models Methods Appl. Sci. 24 (06), 1141–1164.
Morgenstern, Philipp, 2016. Globally structured three-dimensional analysis-suitable T-splines: definition, linear independence and m-graded local refinement. SIAM J. Numer. Anal. 54 (4), 2163–2186.
Morgenstern, Philipp, 2017. Mesh refinement strategies for the adaptive isogeometric method. PhD thesis. University of Bonn.
Morgenstern, Philipp, Peterseim, Daniel, 2015. Analysis-suitable adaptive T-mesh refinement with linear complexity. Comput. Aided Geom. Des. 34, 50–66.
Morin, Pedro, Nochetto, Ricardo H., Siebert, Kunibert G., 2000. Data oscillation and convergence of adaptive FEM. SIAM J. Numer. Anal. 38 (2), 466–488.
Nochetto, Ricardo H., Veeser, Andreas, 2012. Primer of adaptive finite element methods. In: Multiscale and Adaptivity: Modeling, Numerics and Applications. In: Lecture Notes in Mathematics, vol. 2040. Springer, Berlin, Heidelberg, pp. 125–225.
Scott, Michael A., Li, Xin, Sederberg, Thomas W., Hughes, Thomas J.R., 2012. Local refinement of analysis-suitable T-splines. Comput. Methods Appl. Mech. Eng. 213, 206–222.
Sederberg, Thomas W., Zheng, Jianmin, Bakenov, Almaz, Nasri, Ahmad, 2003. T-splines and T-NURCCs. ACM Trans. Graph. 22 (3), 477–484.
Stevenson, Rob, 2007. Optimality of a standard adaptive finite element method. Found. Comput. Math. 7 (2), 245–269.
Verfürth, Rüdiger, 2013. A Posteriori Error Estimation Techniques for Finite Element Methods. Oxford University Press, Oxford.
Vuong, Anh-Vu, Giannelli, Carlotta, Jüttler, Bert, Simeon, Bernd, 2011. A hierarchical approach to adaptive local refinement in isogeometric analysis. Comput. Methods Appl. Mech. Eng. 200 (49), 3554–3567.